

PIERRE  
AUGER  
OBSERVATORY



# Latest Results from the Pierre Auger Observatory

Bruce Dawson  
The University of Adelaide, Australia

Photo: Steven Saffi, University of Adelaide

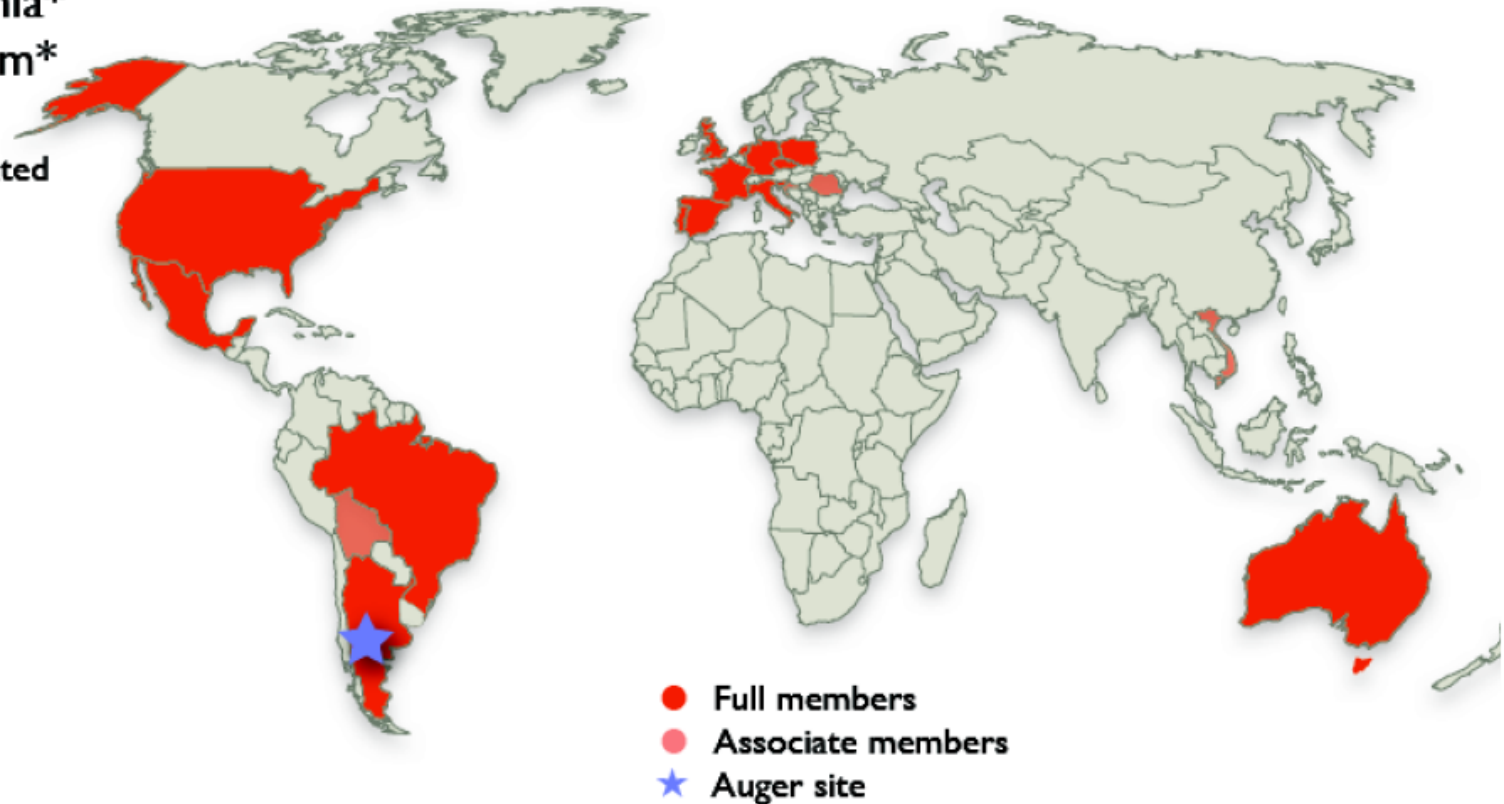


# Pierre Auger Collaboration

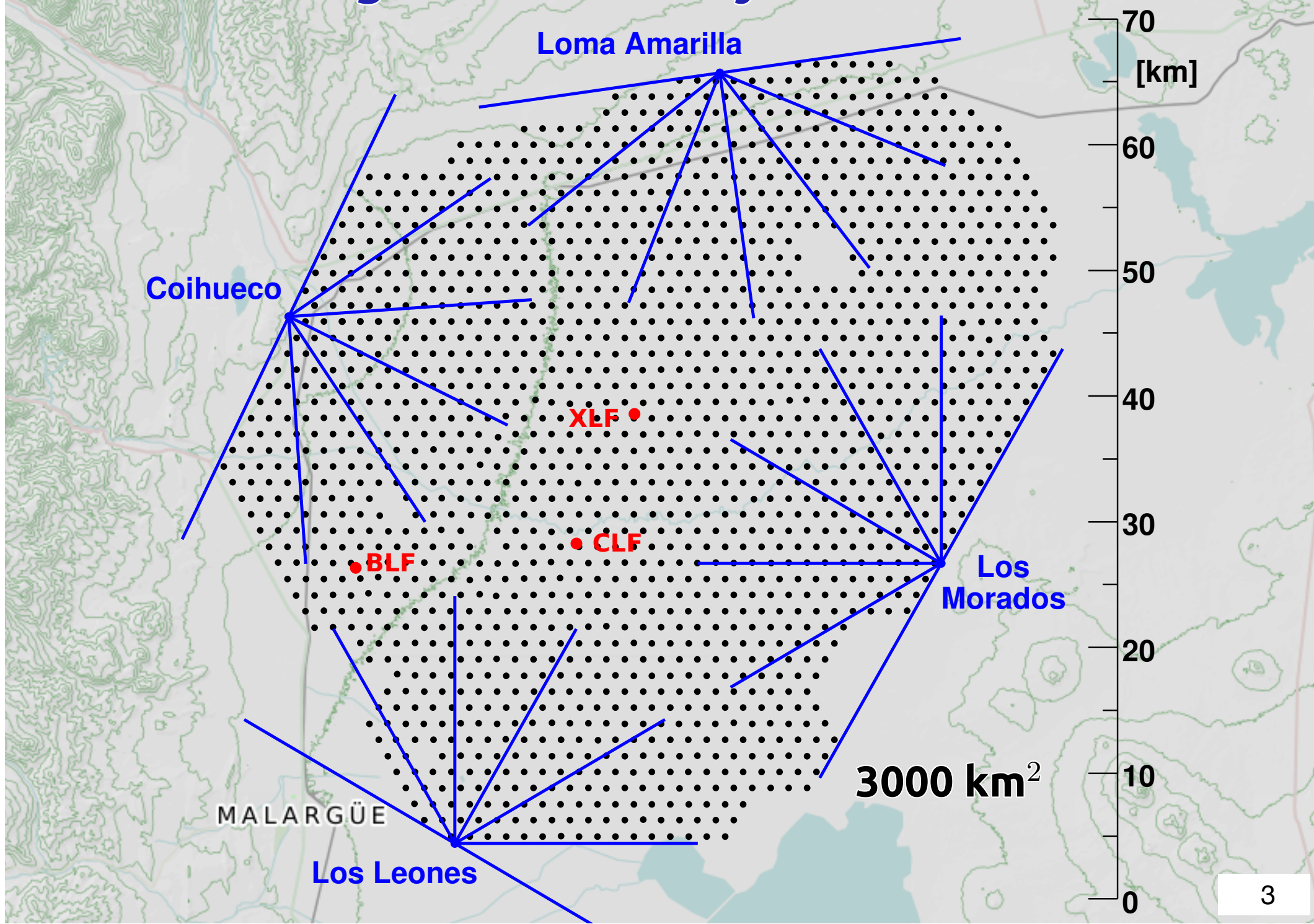
About 500 members from 19 countries

Argentina  
Australia  
Brazil  
Croatia  
Czech Republic  
France  
Germany  
Italy  
Mexico  
Netherlands  
Poland  
Portugal  
Slovenia  
Spain  
United Kingdom  
USA

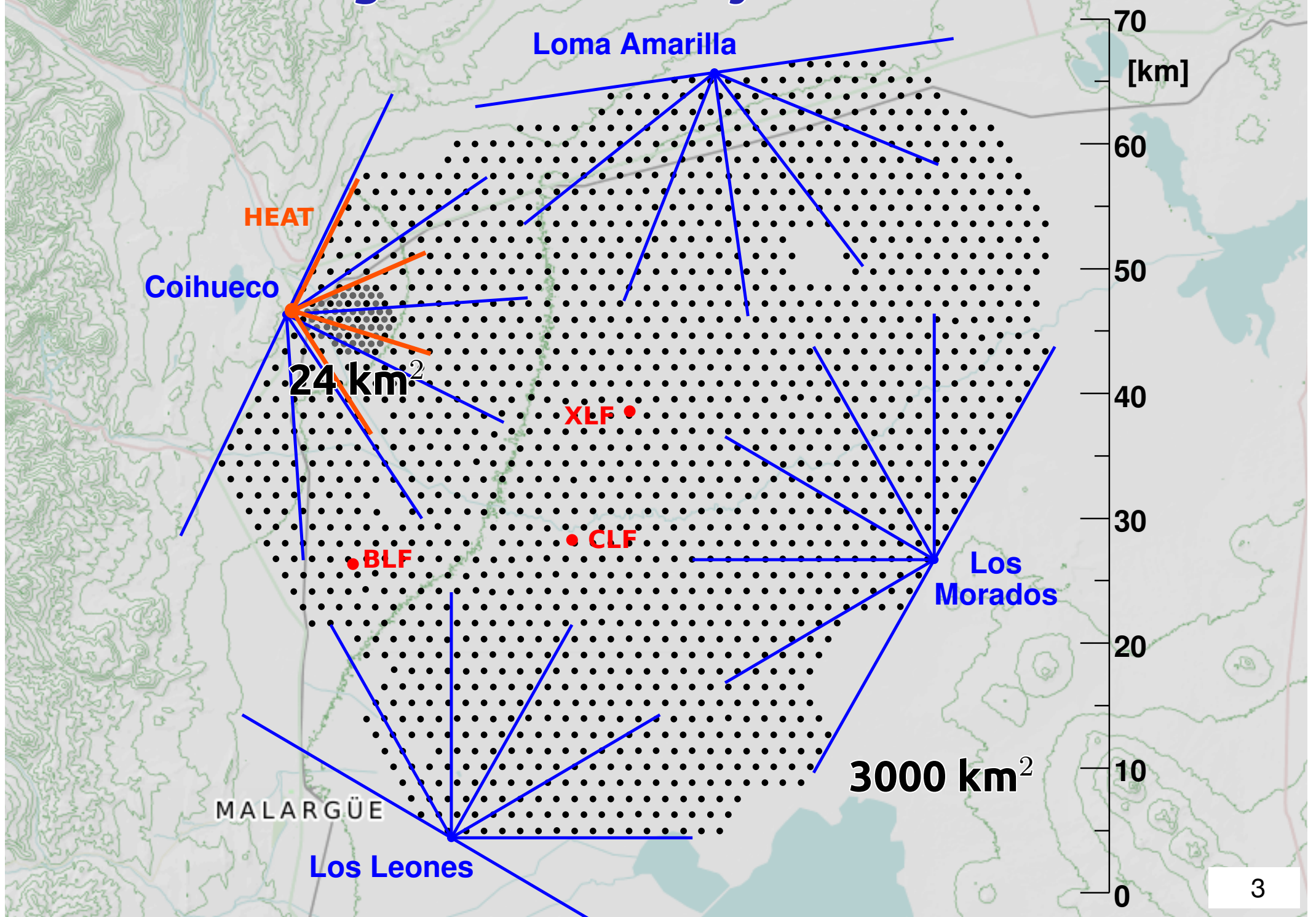
Bolivia\*  
Romania\*  
Vietnam\*  
  
\*Associated



# The Pierre Auger Observatory



# The Pierre Auger Observatory



# Pierre Auger Observatory

## Fluorescence Detector

UV light from excited  $N_2$

4 x 6 telescopes,  $30^\circ \times 30^\circ$

+ 3 high-elevation telescopes

## Surface Detector Array

charged particle + photon detector

1500 m grid: 1700 stations (3000 km<sup>2</sup>)

+ 750 m grid: 71 stations, (25 km<sup>2</sup>)

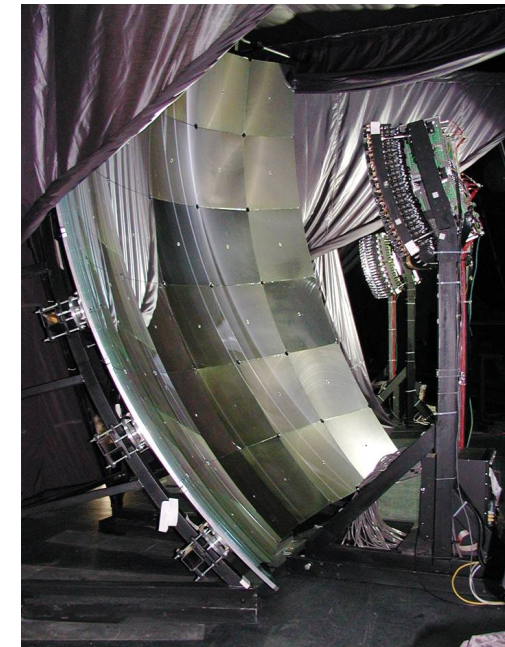
Auger Anisotropy ICRC17:  $9.0 \times 10^4$  km<sup>2</sup> sr yr

Auger Spectrum ICRC17:  $6.7 \times 10^4$  km<sup>2</sup> sr yr

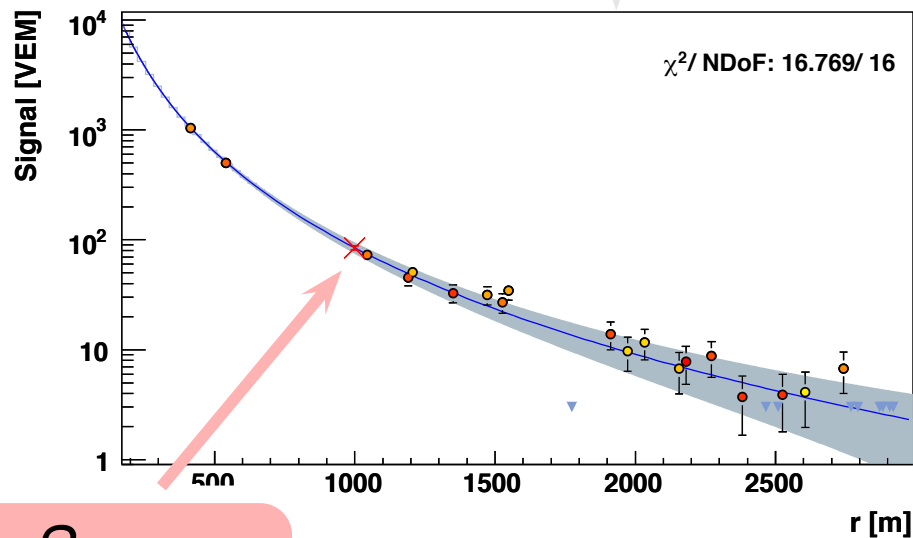
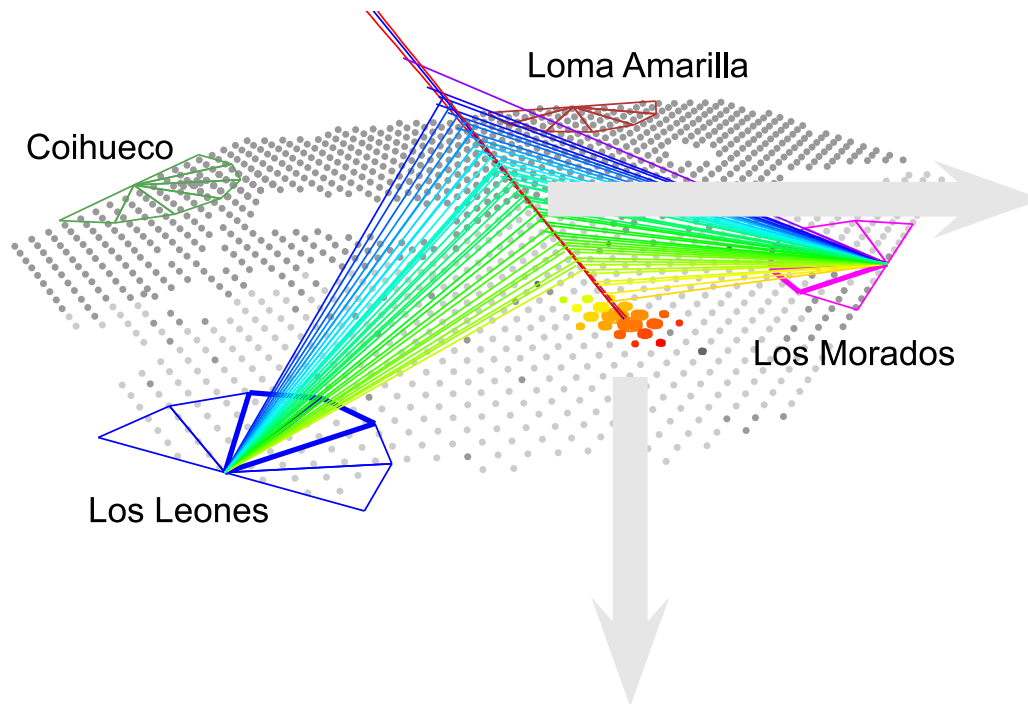
TA Spectrum ICRC17:  
 $0.8 \times 10^4$  km<sup>2</sup> sr yr

AGASA

Exposure dominated by SD array.

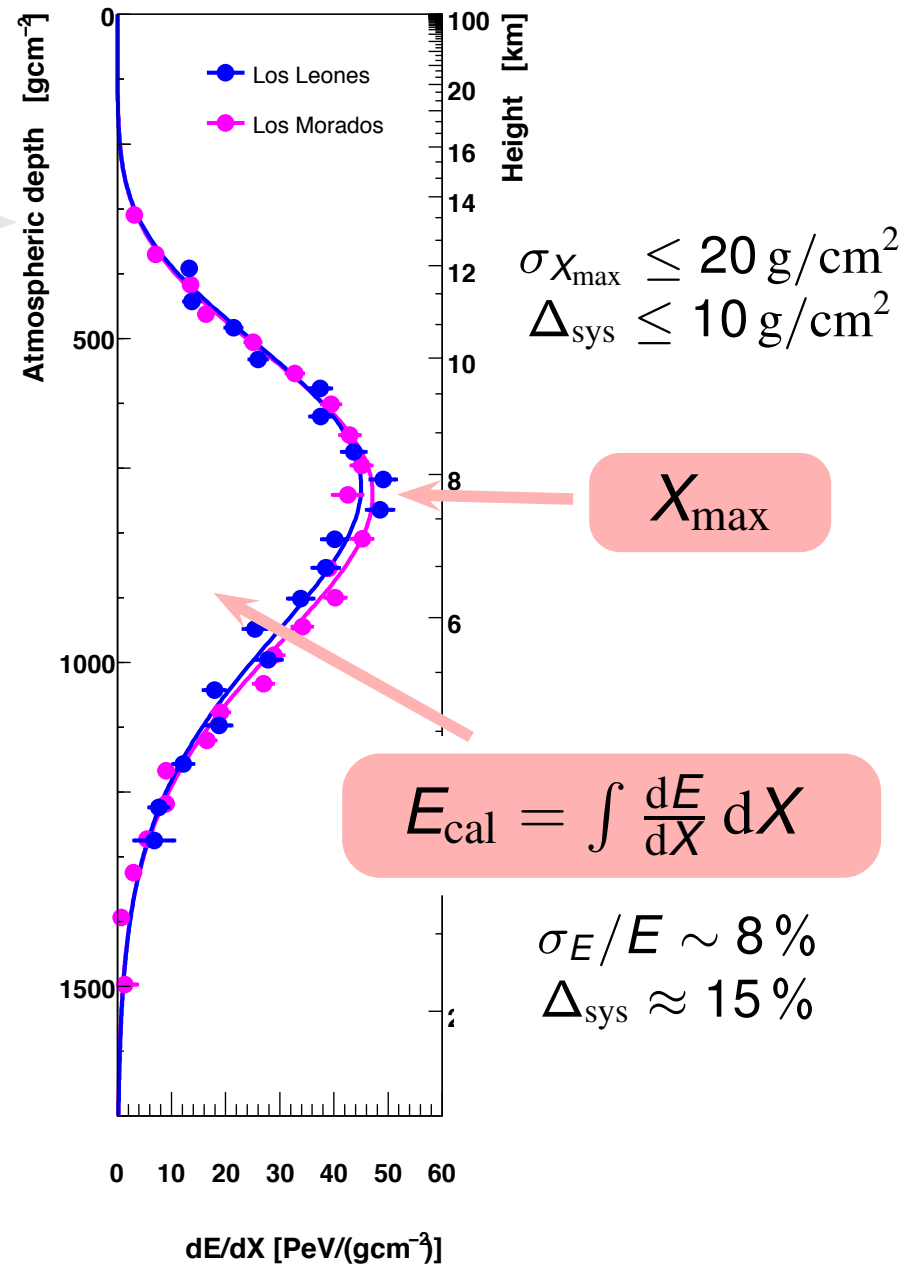


# Auger is a Hybrid detector - FD calibrates SD energy scale

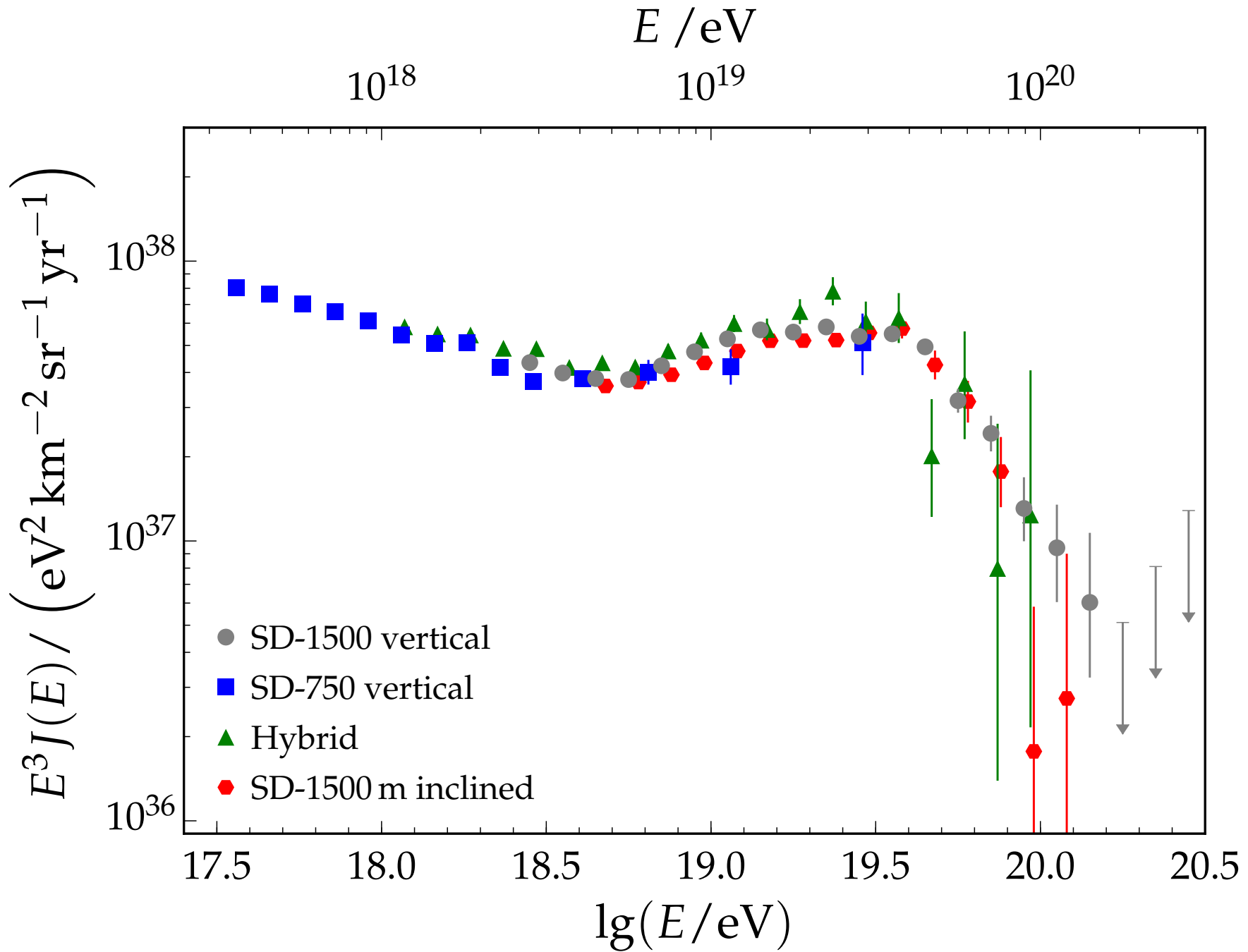


$S_{1000}$

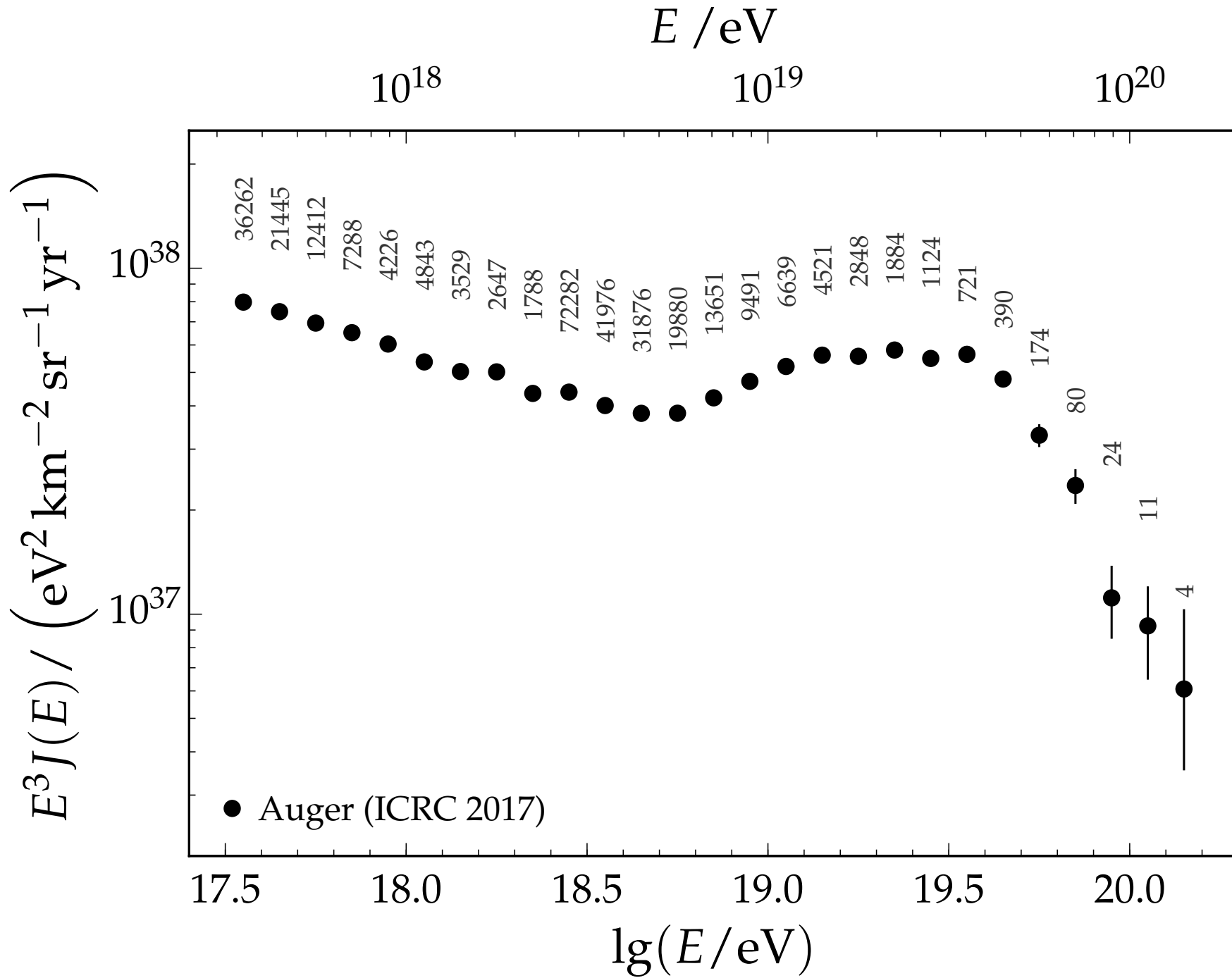
$$E_{\text{surface}} = f(S_{1000}, \theta)$$



# Energy Spectrum

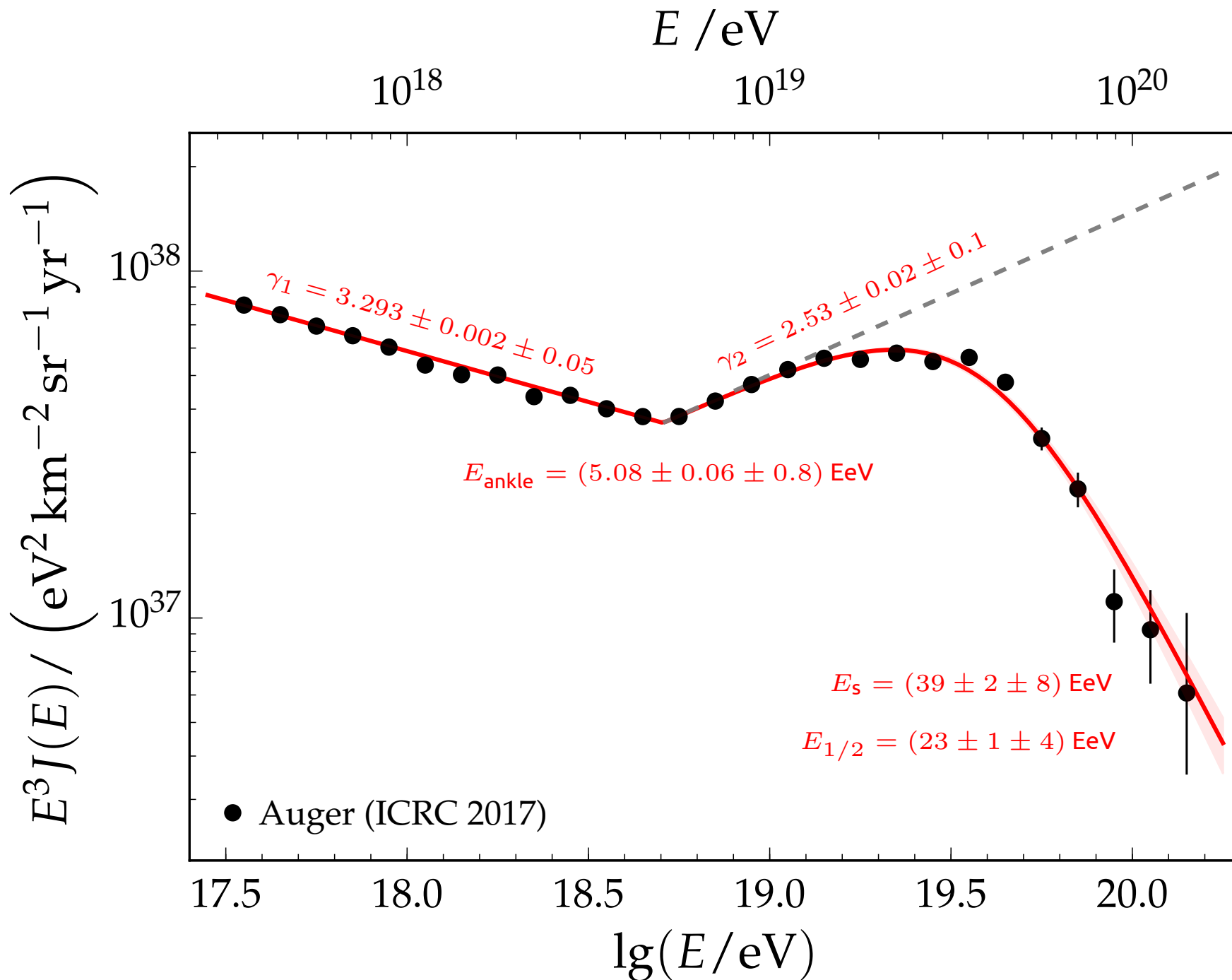


# Combined Energy Spectrum

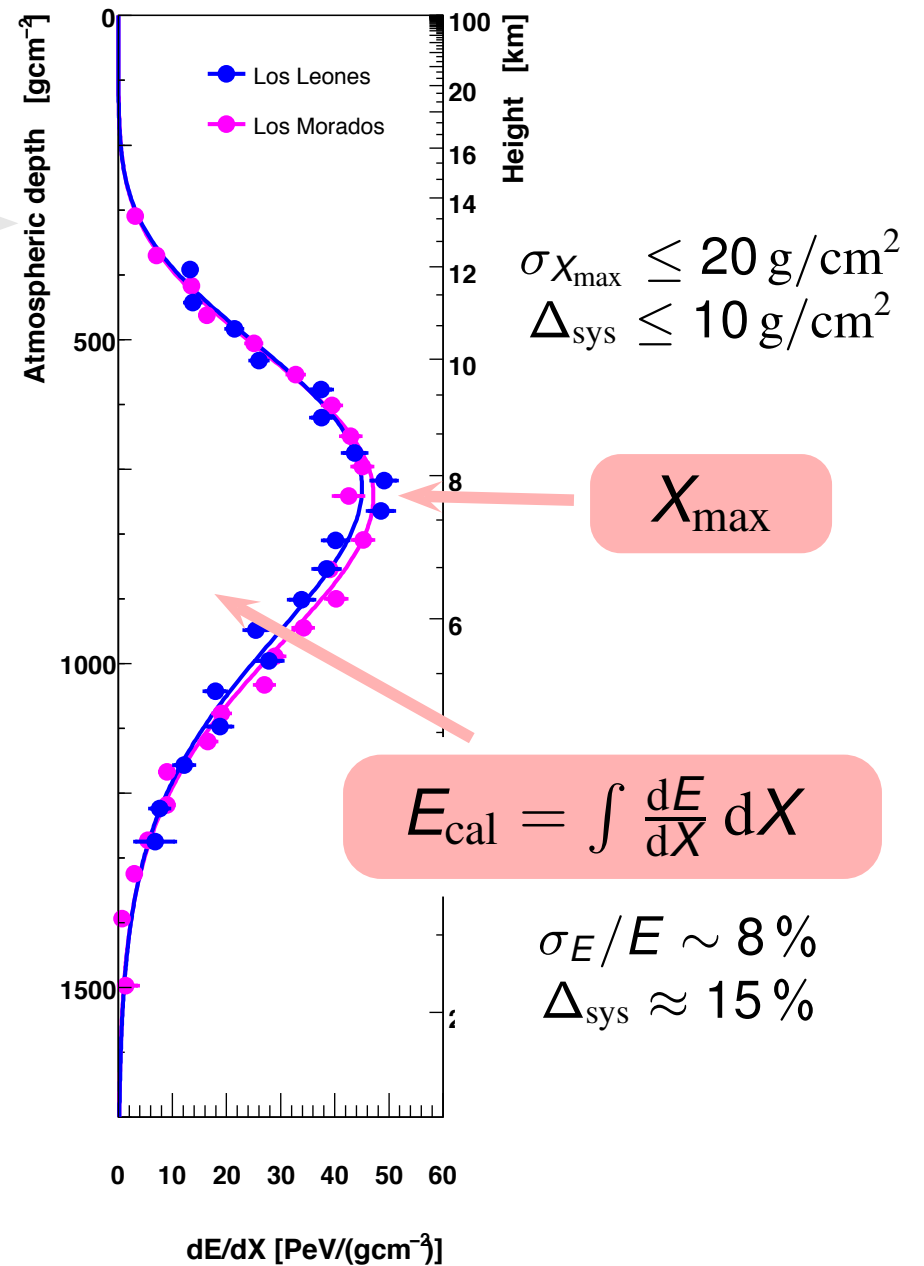
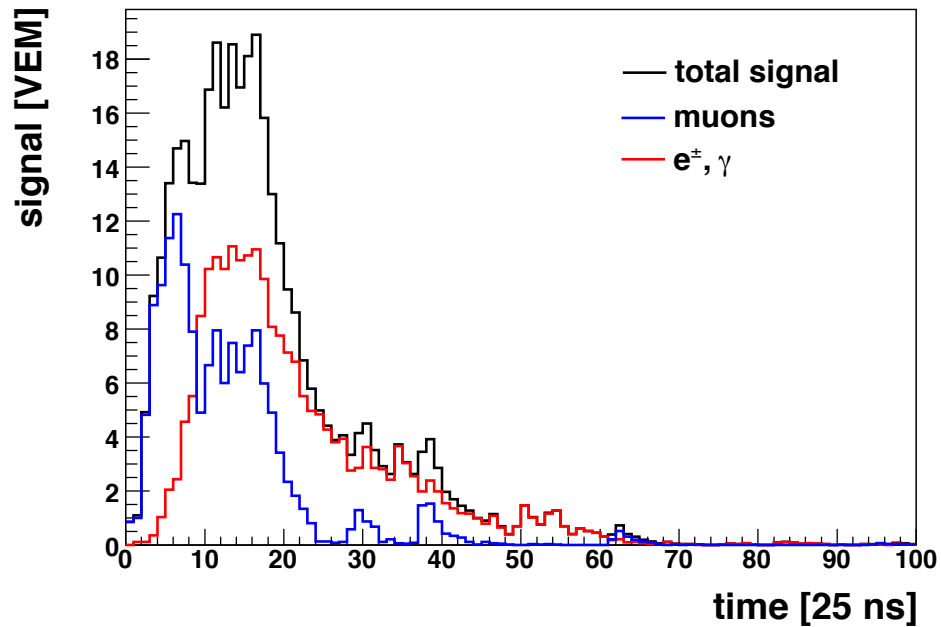
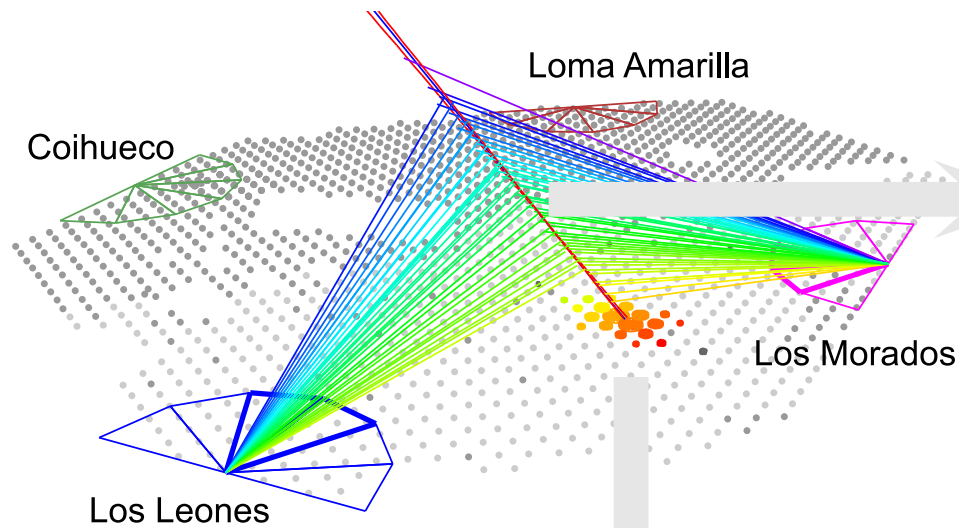




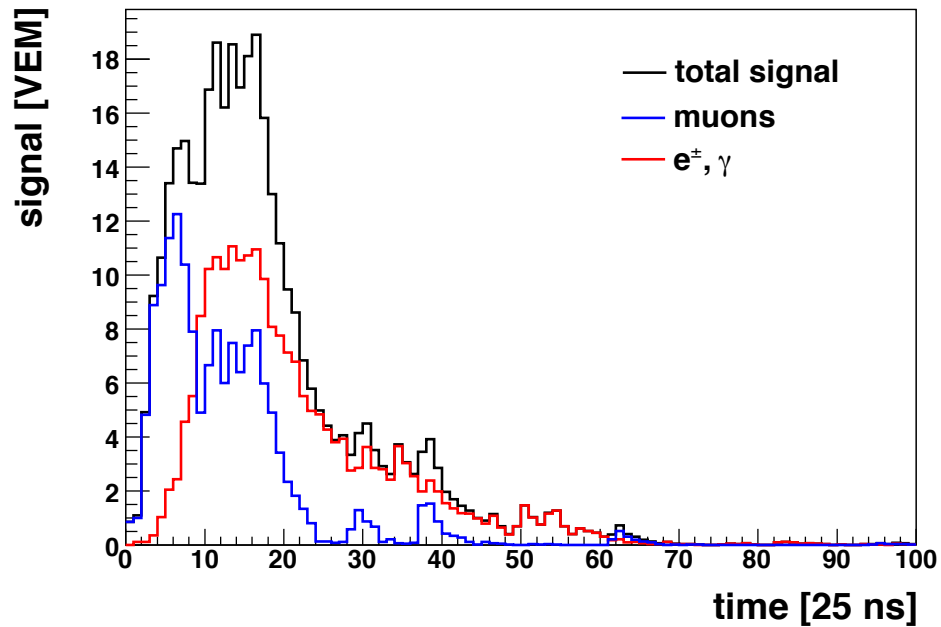
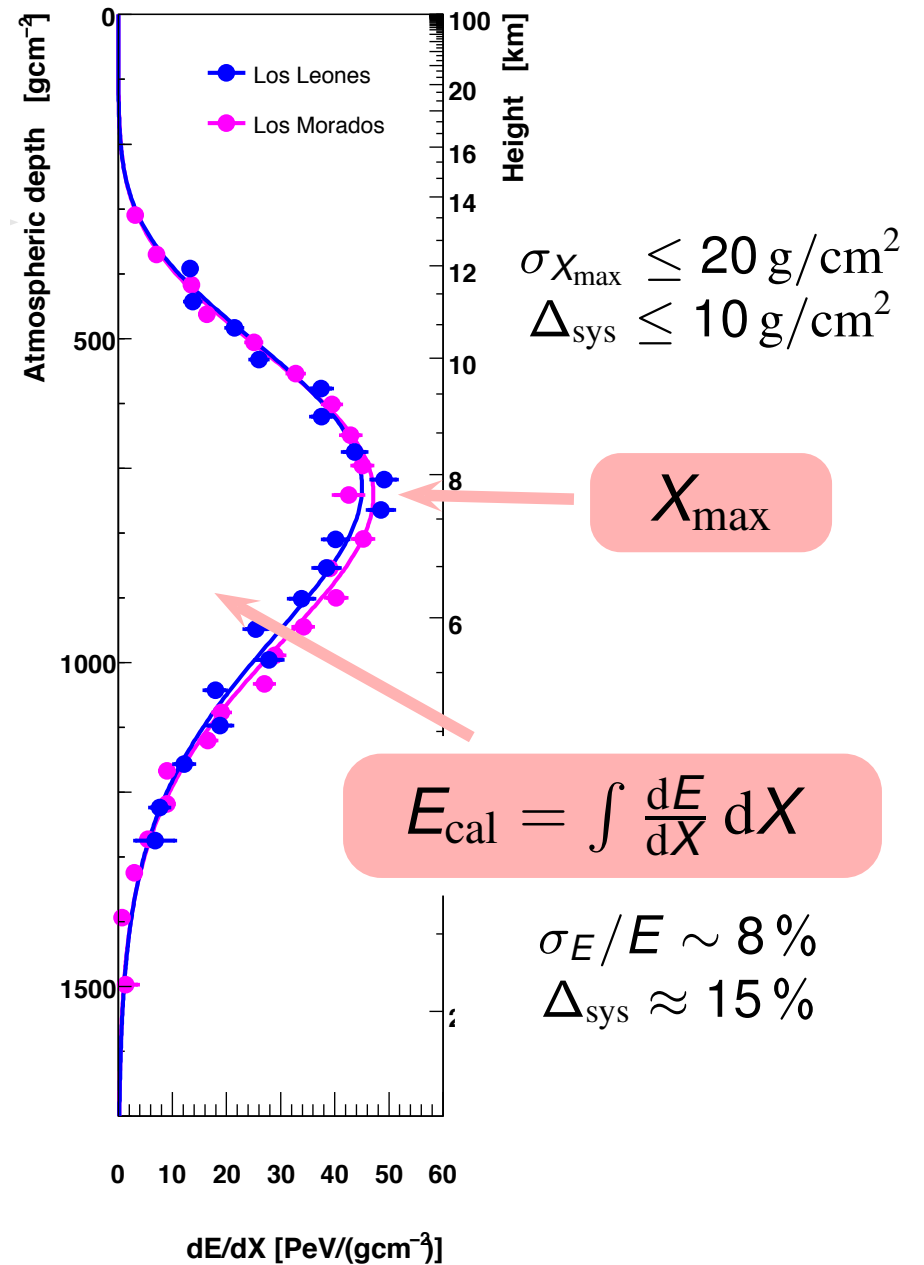
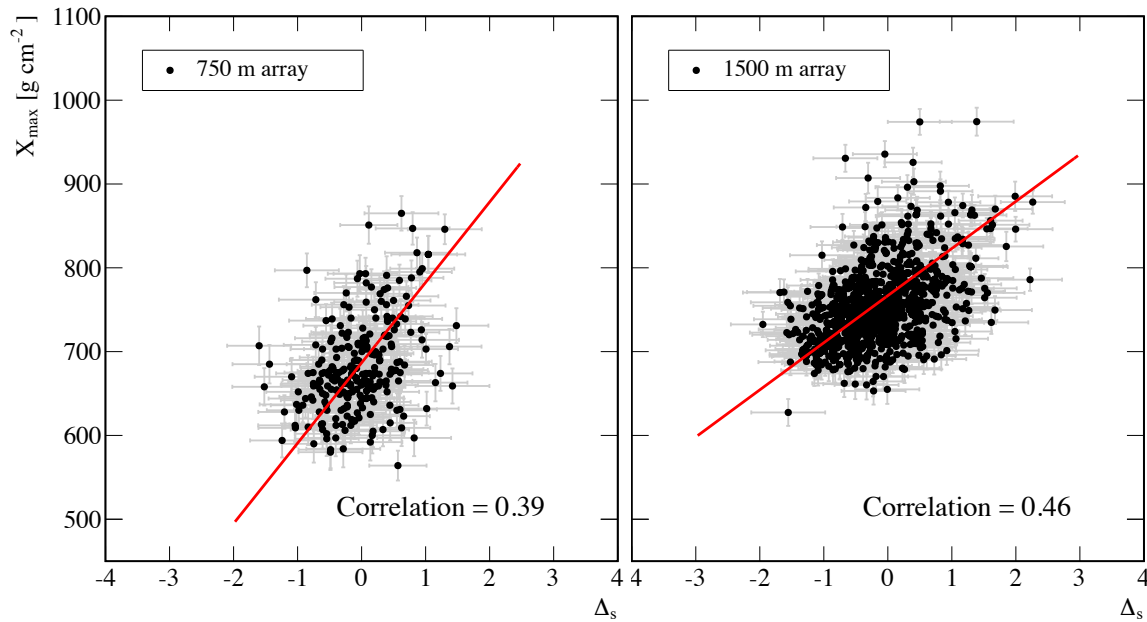
# Combined Energy Spectrum



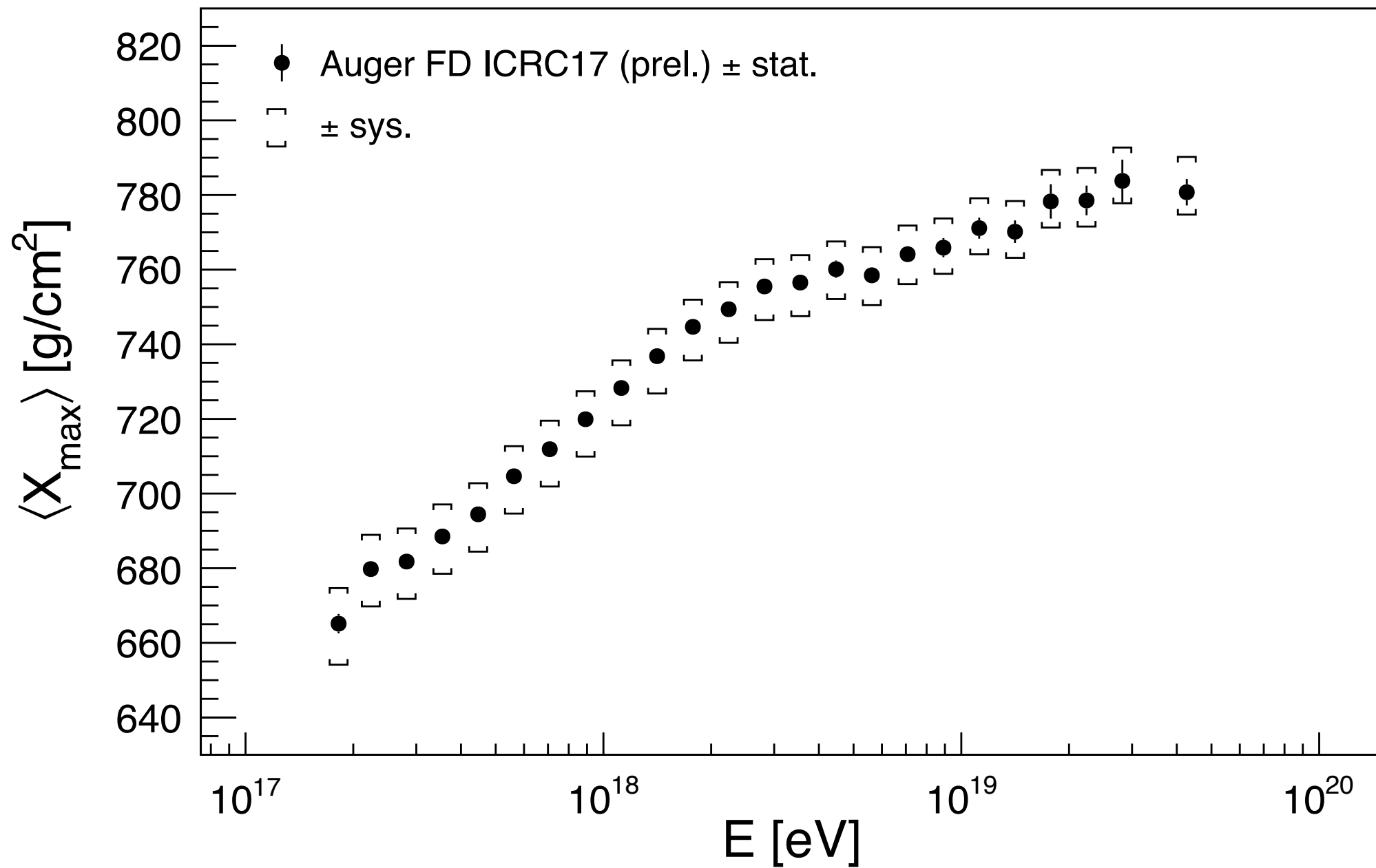
# Mass composition



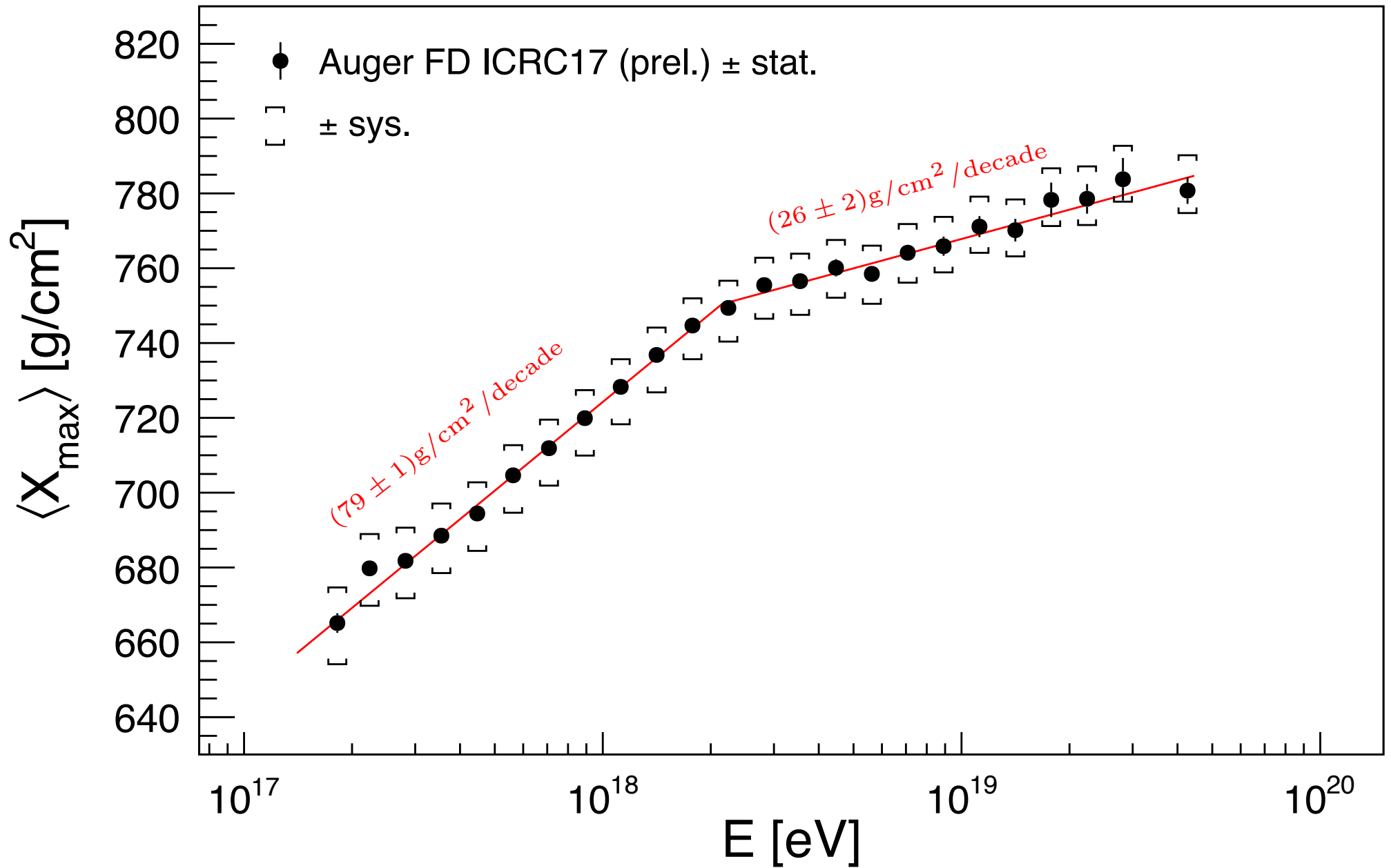
# Mass composition



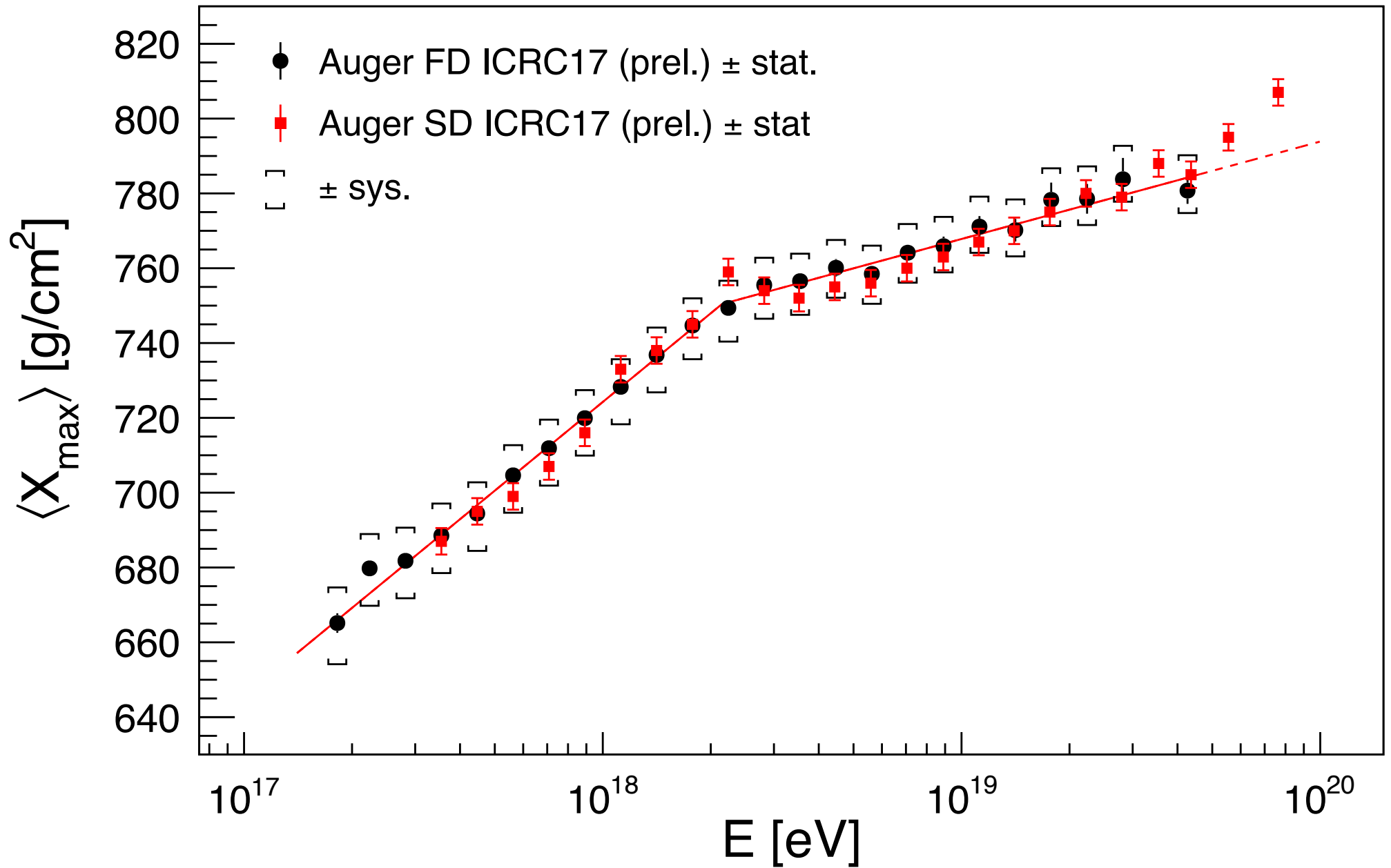
# Mean $X_{\max}$ from fluorescence detectors



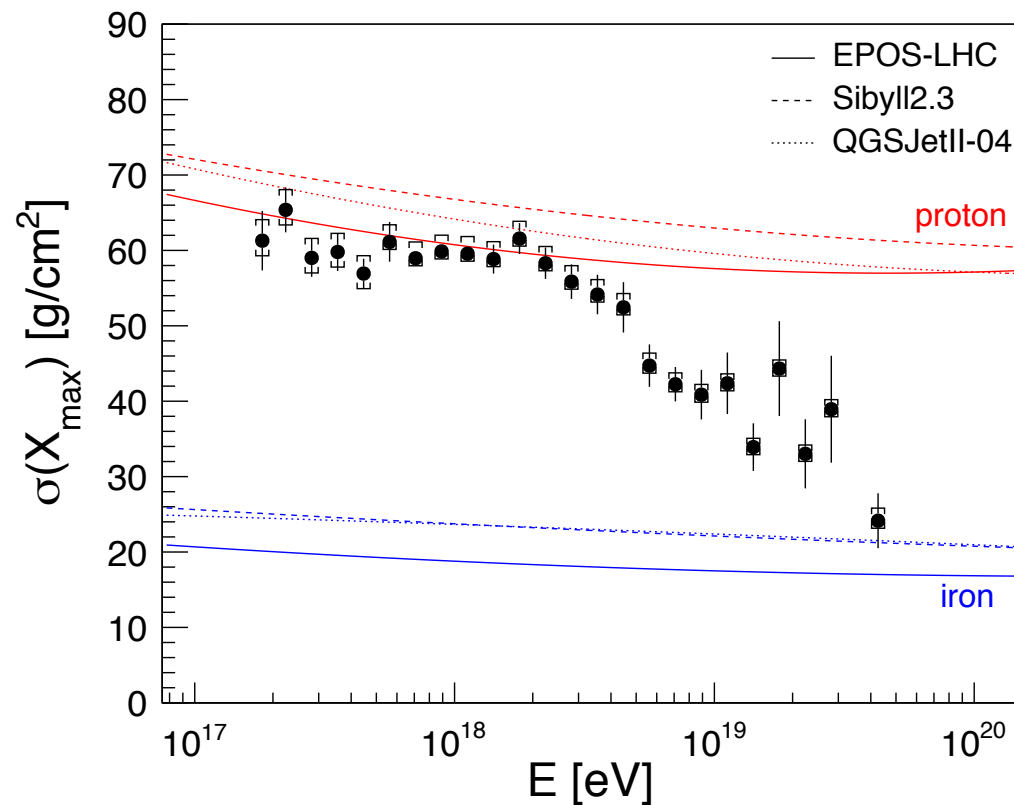
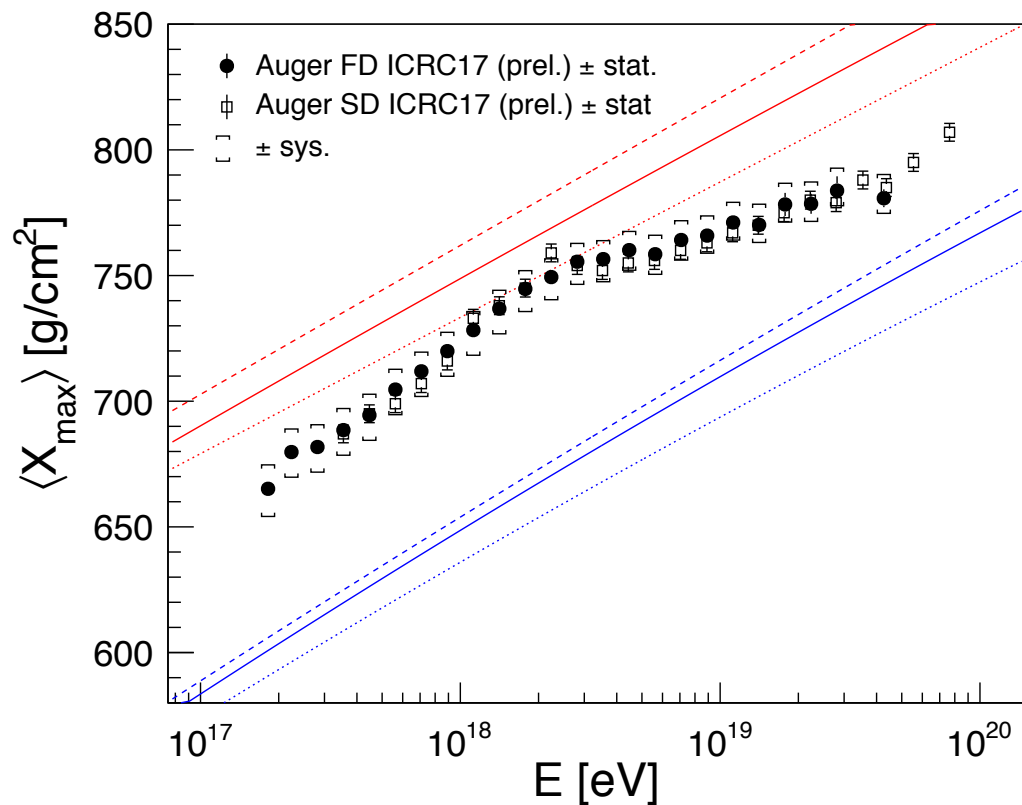
# Mean $X_{\max}$ from fluorescence detectors



# Mean $X_{\max}$ from fluorescence and surface detectors



# Mean $X_{\max}$ and fluctuations in $X_{\max}$ (latter from from fluorescence detectors only)

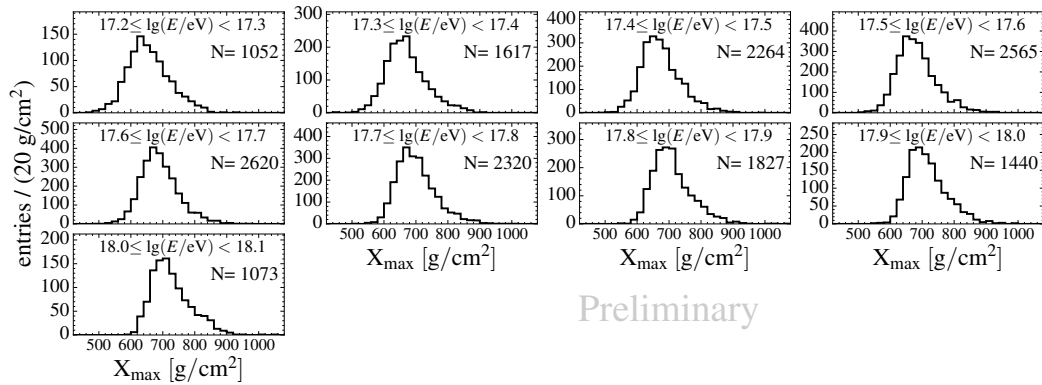


lines: air shower simulations using post-LHC hadronic interaction models

# Fits of full $X_{\max}$ distributions with (p-He-N-Fe) mixtures

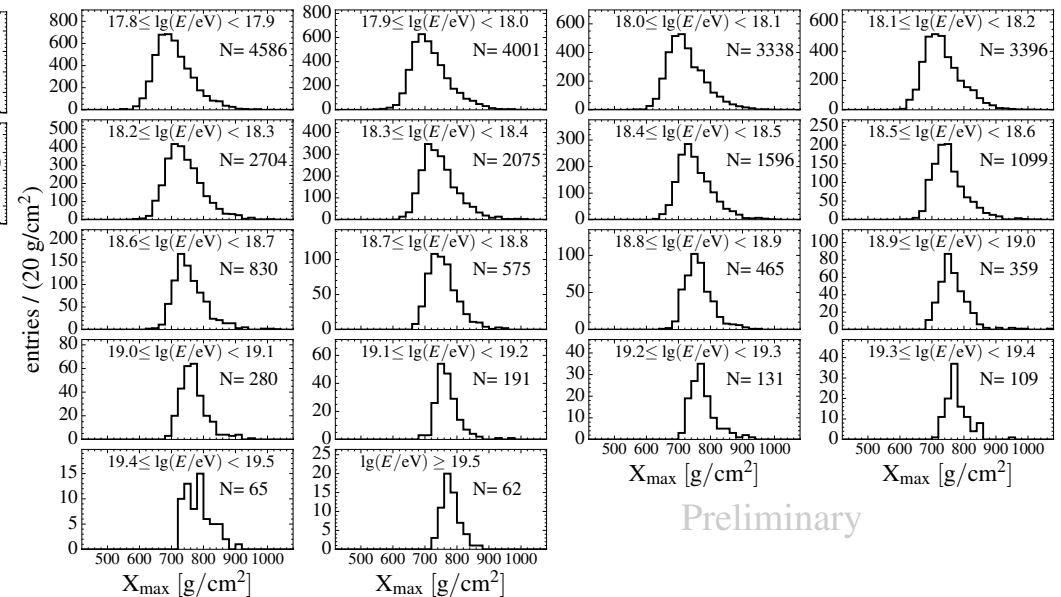
From FD

$\lg(E/\text{eV}) = 17.2 \dots 18.1$



Preliminary

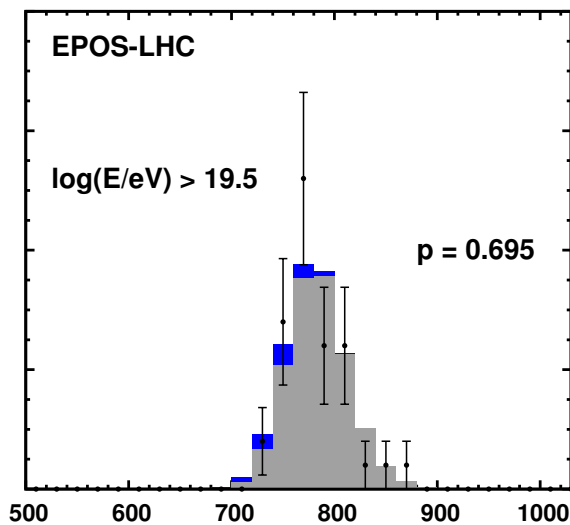
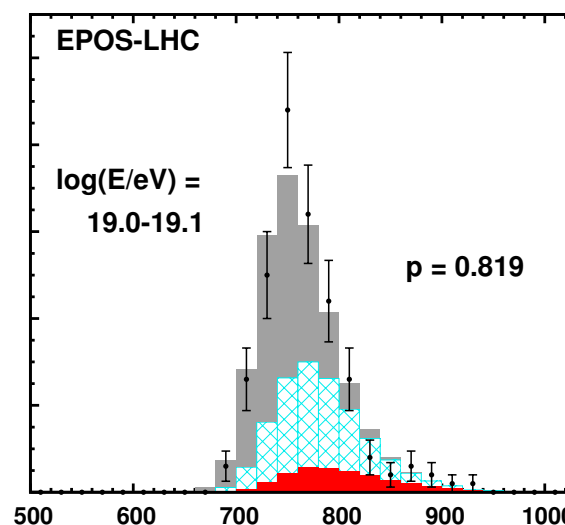
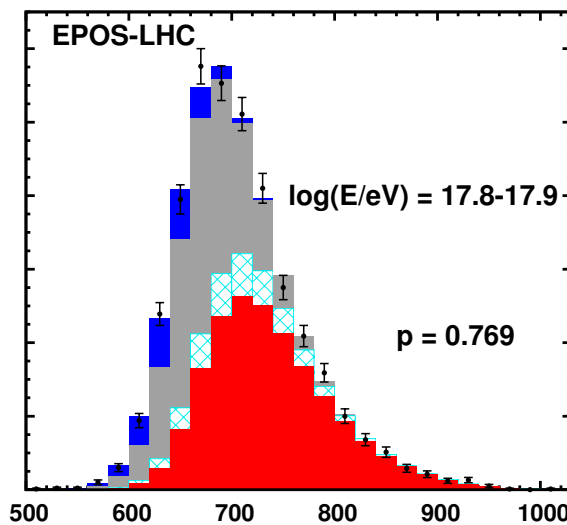
$\lg(E/\text{eV}) = 17.8 \dots > 19.5$



Preliminary

Examples of 4-component fit:

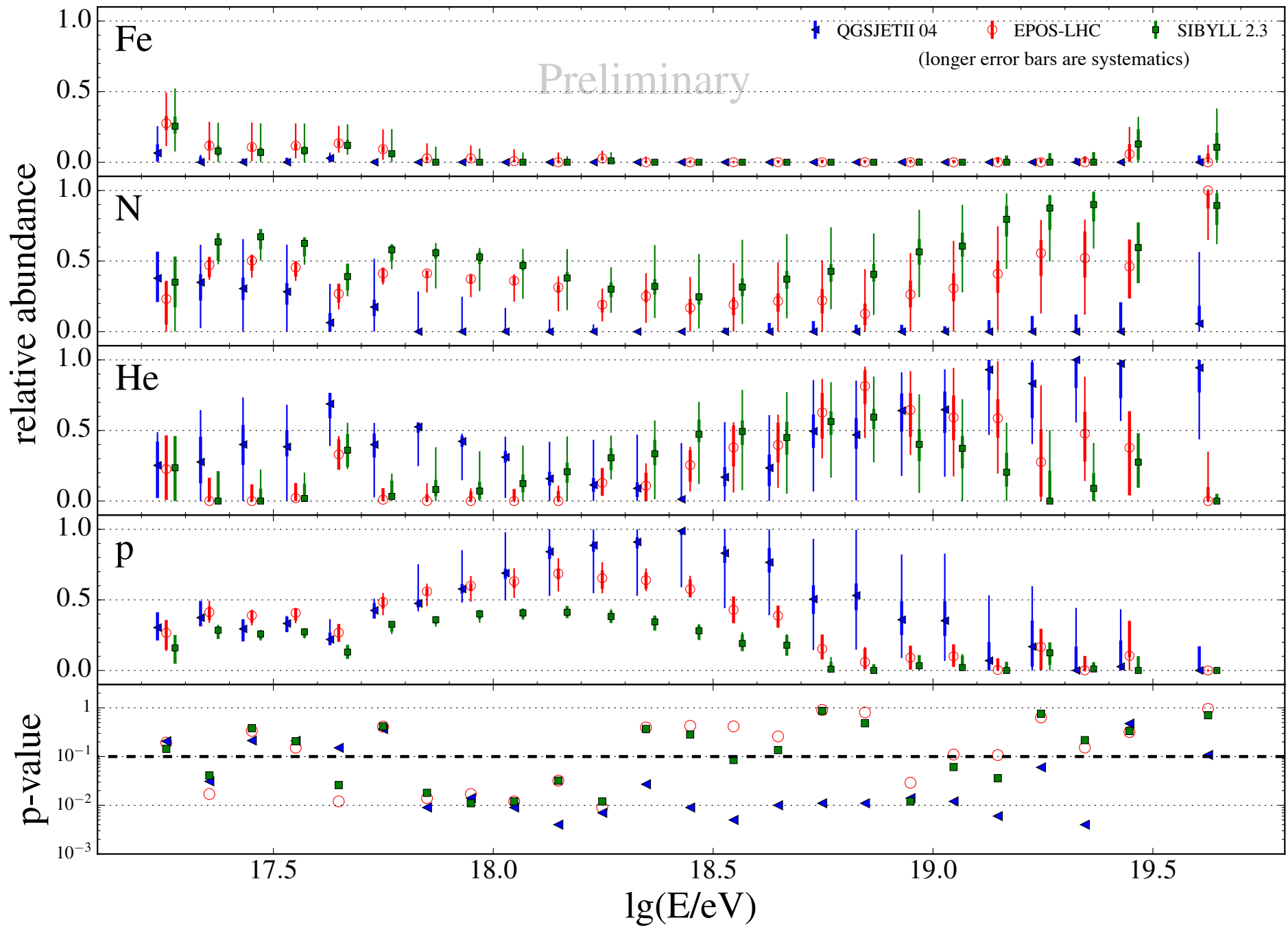
p He N Fe



$X_{\max} [\text{g}/\text{cm}^2]$



# Mass fractions



# Astrophysical interpretation: very simple models

Simulate propagation of CR particles in cosmic photon fields

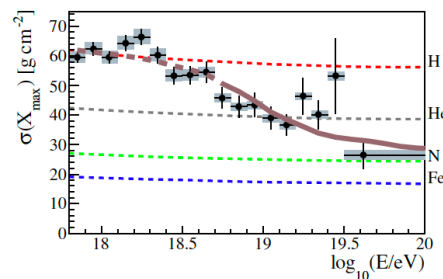
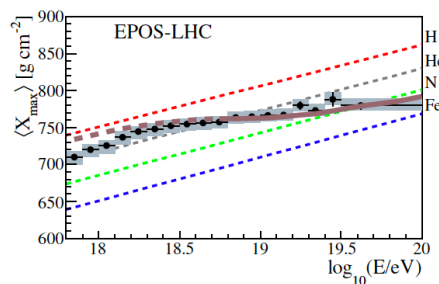
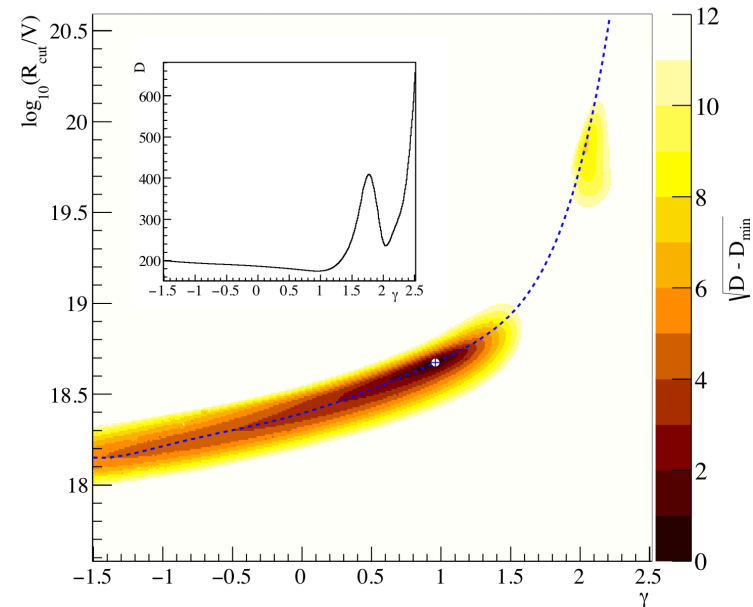
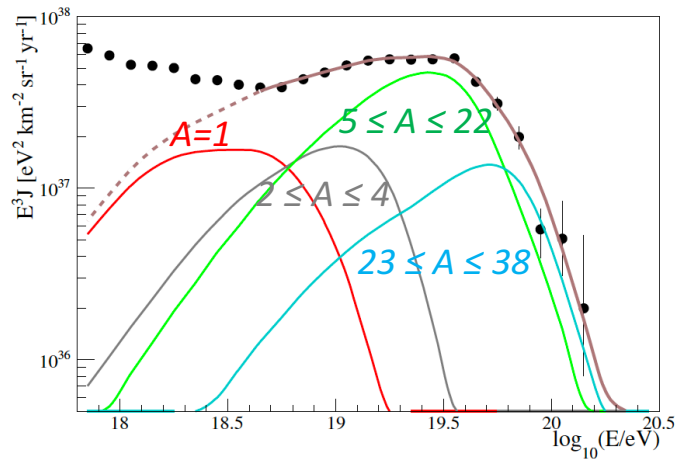
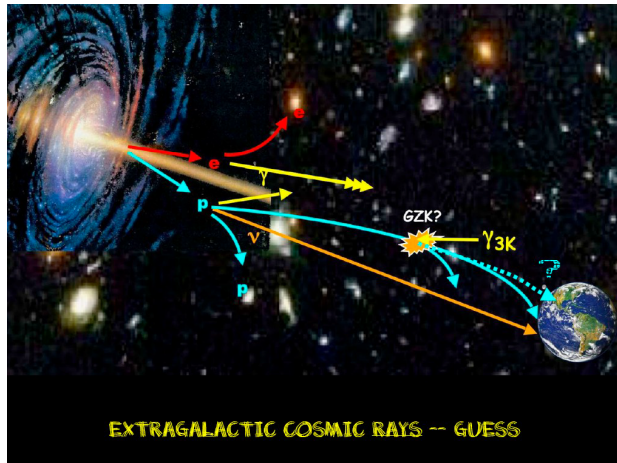
- match to measured spectrum and mass composition at Earth
- 1D propagation through photon fields
- Homogeneous distribution of identical sources of p, He, N, (Si), Fe
- CR injection = power law + rigidity cutoff

Similar scenarios studied by Aharonian, Ahlers, Allard, Aloisio, Berezhinsky, Blasi, Hooper, Olinto, Parizot, Taylor, ...

Results: hard/very hard injection spectrum unless nearby sources assumed.

Full study incl. model and data uncertainties:

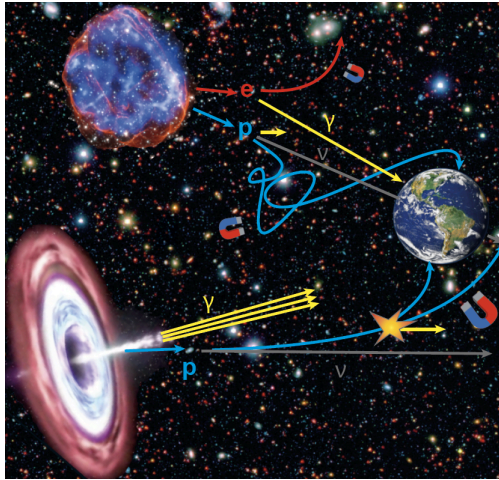
Aab et al. [Auger Collab.] JCAP (2017) 1704, 038.



$$\frac{dN}{dE} = J_0 \sum_{\alpha} f_{\alpha} E_0^{-\gamma} \begin{cases} 1 & \text{for } E_0/Z_{\alpha} < R_{\text{cut}} \\ \exp\left(1 - \frac{E_0}{Z_{\alpha} R_{\text{cut}}}\right) & \text{for } E_0/Z_{\alpha} \geq R_{\text{cut}} \end{cases}$$

“Reference” model: SimProp, PSB x-sect, Gilmore '12 EBL, EPOS-LHC

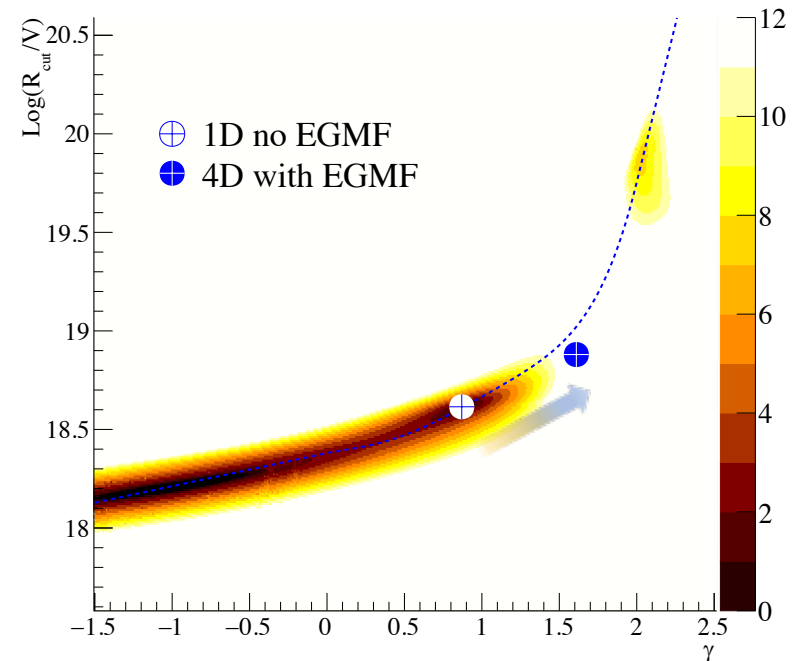
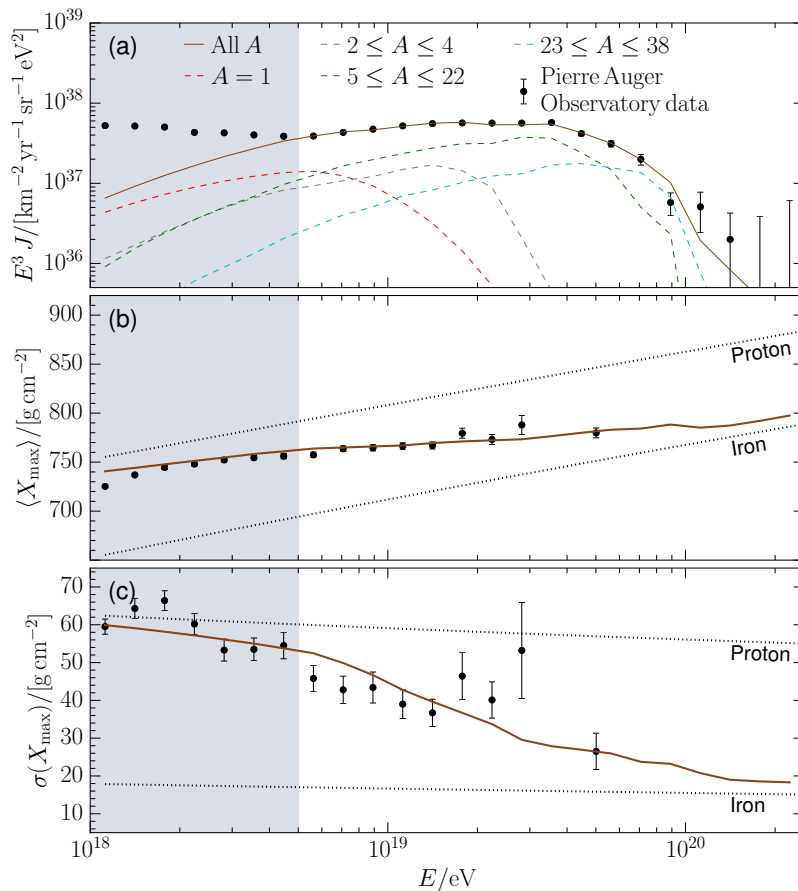
# Astrophysical interpretation: adding some extra reality



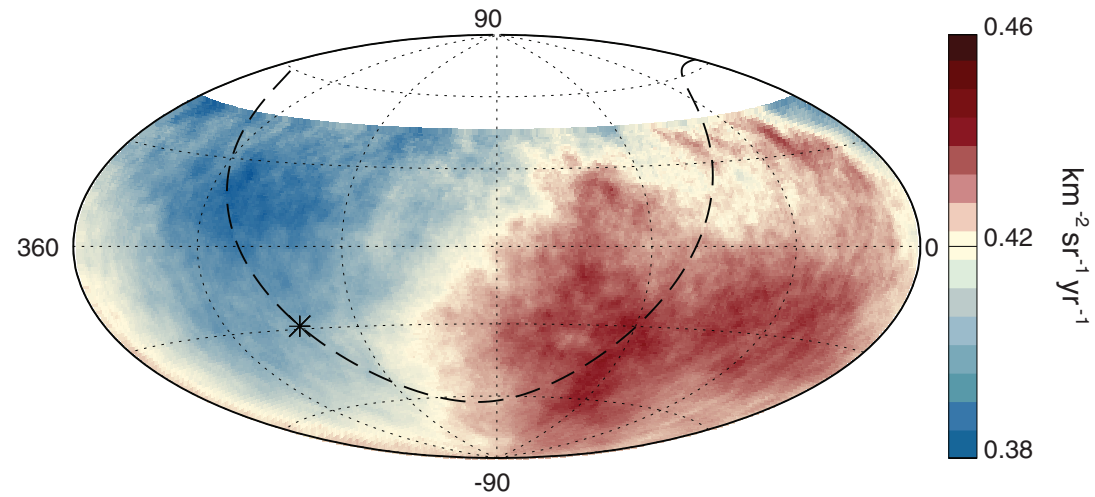
- e.g. Wittkowski [Auger Collab.] ICRC 2017
- 4D propagation (incl. source evolution) with CRPropa3
- extragalactic B fields, large scale structure (Dolag `12), Gilmore `12 EBL, EPOS-LHC

Source properties	4D with EGMF	4D no EGMF	1D no EGMF <sup>1</sup>
$\gamma$	1.61	0.61	0.87
$\log_{10}(R_{\text{cut}}/\text{eV})$	18.88	18.48	18.62
$f_{\text{H}}$	3 %	11 %	0 %
$f_{\text{He}}$	2 %	14 %	0 %
$f_{\text{N}}$	74 %	68 %	88 %
$f_{\text{Si}}$	21 %	7 %	12 %
$f_{\text{Fe}}$	0 %	0 %	0 %

previous slide



# Anisotropy



# Indication of Intermediate-scale Anisotropy

A. Aab et al. [Auger Collab.] ApJ. Lett. **833** (2018) L29

## Analysis strategy:

- arrival direction data,  $D$

- sky model from source candidates,  $M_i$

$$M_i = (\text{flux model}) \times (\text{attenuation model}) \times (\text{angular smearing}) \times (\text{exposure})$$

- null hypothesis: isotropy  $M_0$

- single population signal model

$$M = (1 - \alpha)M_0 + \alpha M_i$$

- test statistic:

- ratio of likelihoods of model-data comparison

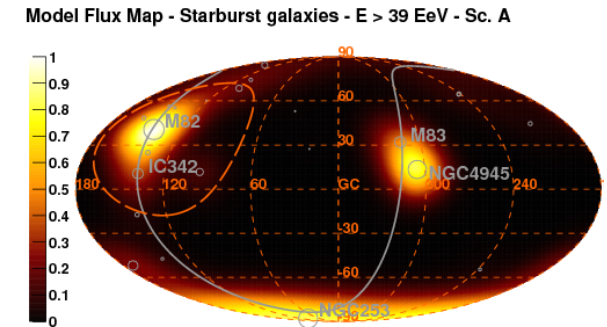
$$TS = 2 \ln \left( P(D|M)/P(D|M_0) \right)$$

think:  $\Delta\chi^2$  of (isotropy + signal) vs isotropy

- $p$ -value from Wilks' theorem:  $p(TS) = p_{\chi^2}(TS, \Delta\text{ndf})$

- a large TS means

- $M$  describes  $D$  much better than  $M_0$
- $M_0$  excluded at  $p$  (not:  $M$  “proven” at  $p$ )



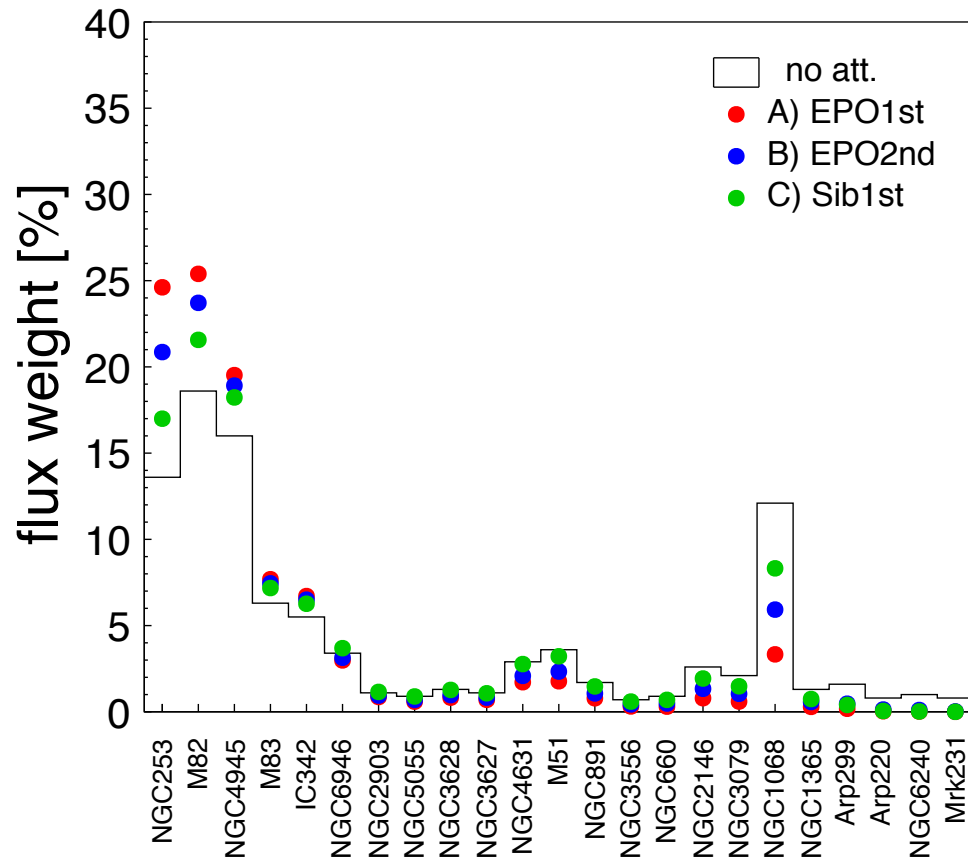


- ▶ **Swift-BAT X-ray-selected galaxies**,  $D < 250$  Mpc,  $\Phi > 1.3 \cdot 10^{-11} \frac{\text{erg}}{\text{cm}^2 \text{s}}$ ,  $w : 14\text{-}195$  keV
- ▶ **2MRS IR-selected galaxies**,  $D > 1$  Mpc,  $w : \text{K-band}$
- ▶ **SBG: 23 nearby starburst galaxies**,  $\Phi > 0.3$  Jy,  $w : \text{radio at } 1.4 \text{ GHz}$
- ▶  **$\gamma$ AGN: 17 2FHL blazars and radio galaxies**,  $D < 250$  Mpc,  $w : \gamma\text{-ray } 50 \text{ GeV-}2 \text{ TeV}$ .

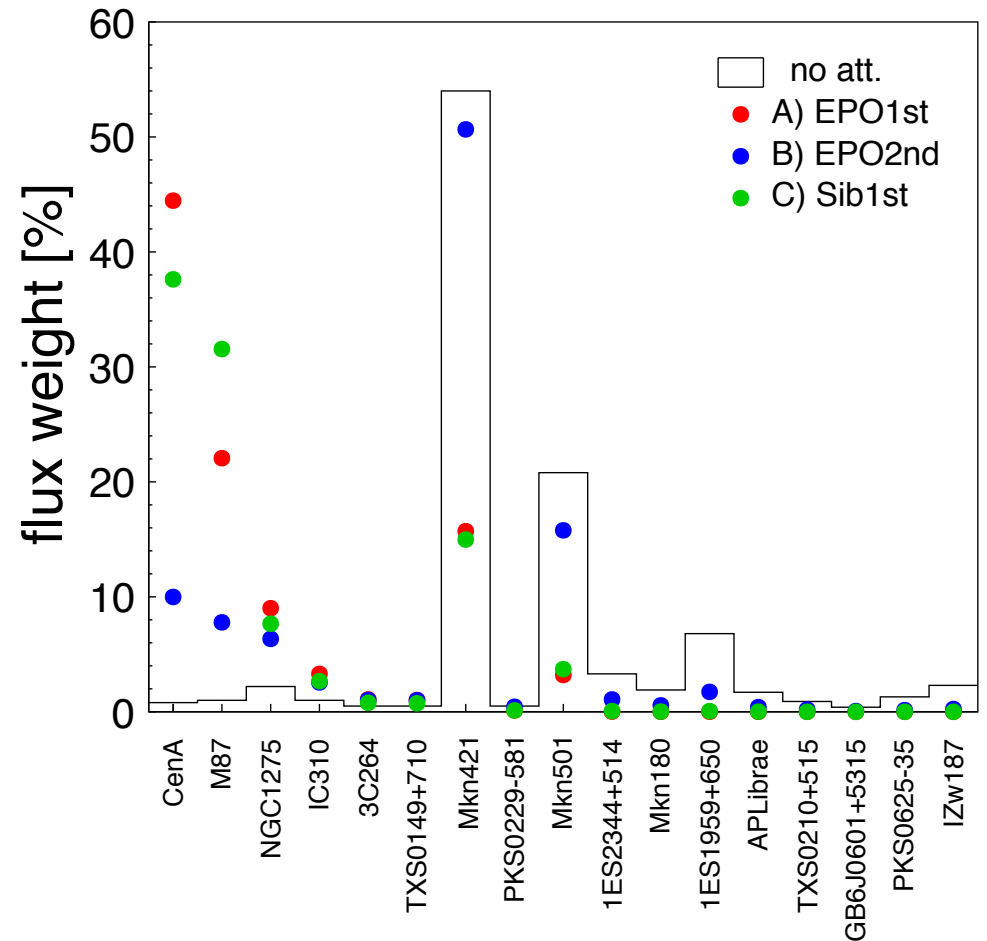
$w$  : UHECR flux proxy, *Swift*-BAT and 2MRS previously tested (ApJ **804** (2015) 172), extragal.  $\gamma$ -ray sources  $\gamma$ AGN and SBG.

# Flux attenuation: depends on mass fractions, distance

starburst



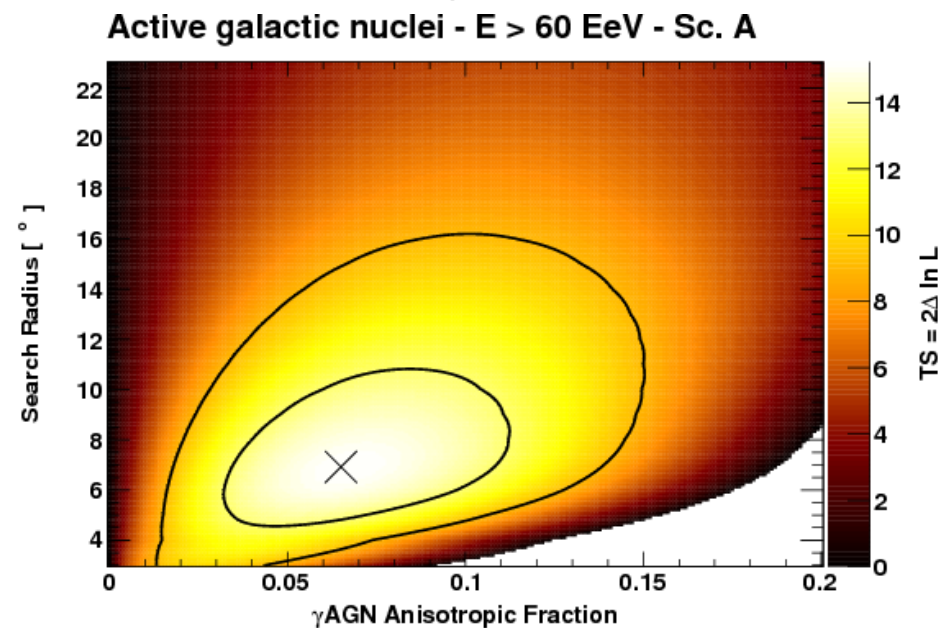
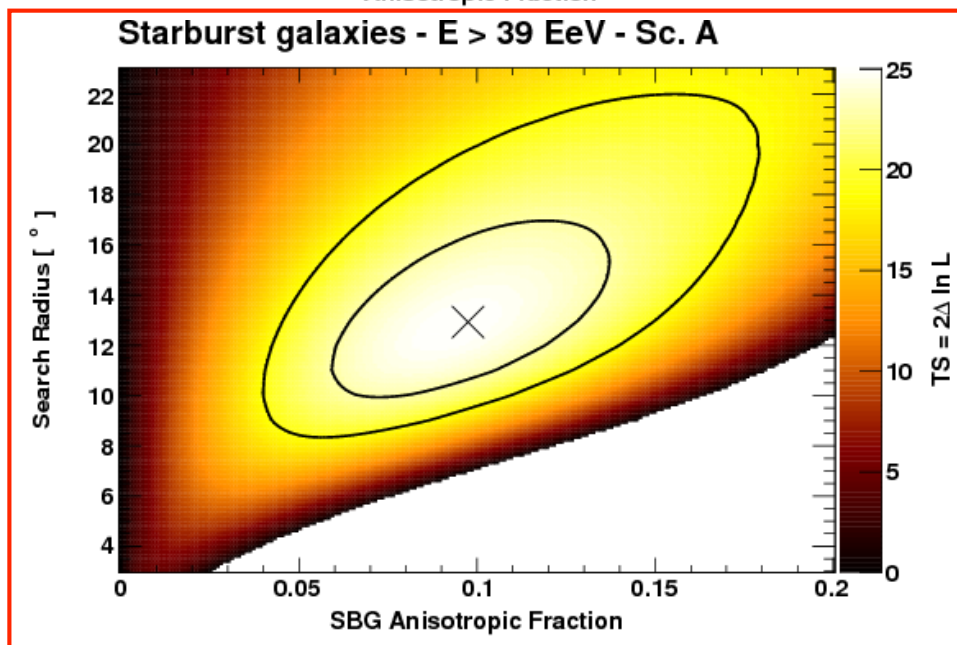
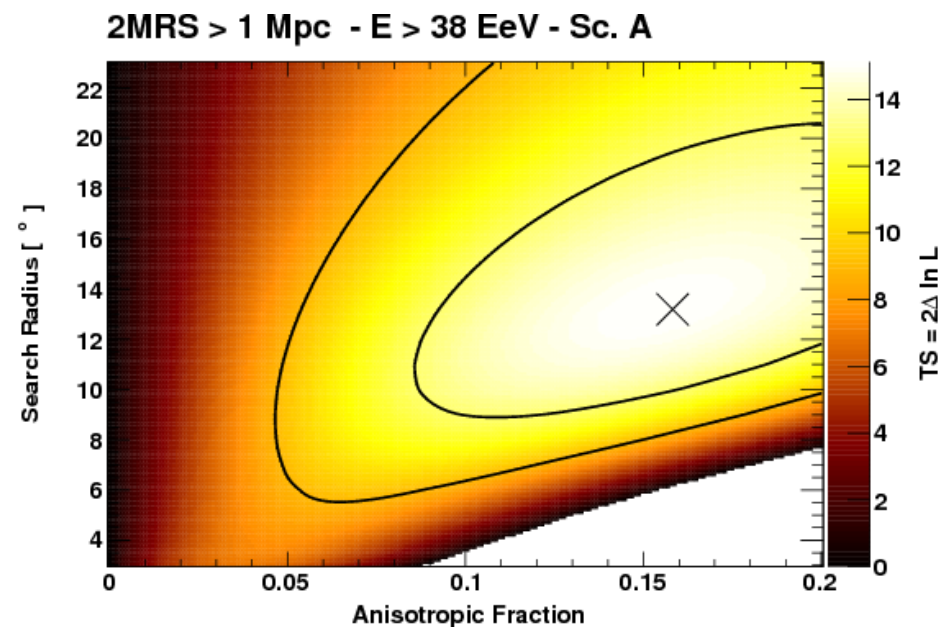
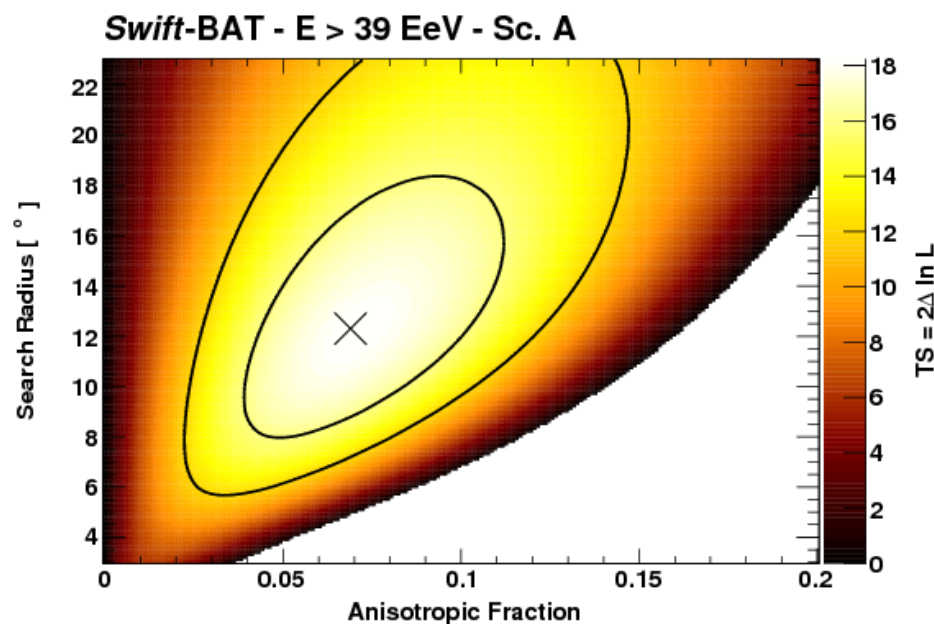
$\gamma$ AGN



composition scenarios from Pierre Auger Coll., JCAP **1704** (2017) 038 + CRPropa3

name	$\lg(R_{\max}/V)$	$f_p$	$f_{\text{He}}$	$f_{\text{N}}$	$f_{\text{Si}}$	$\gamma$
EPO1st	18.68	0.000	0.673	0.281	0.046	0.96
EPO2nd	19.88	0.000	0.000	0.798	0.202	2.04
Sib1st	18.28	0.702	0.295	0.003	0.000	-1.50

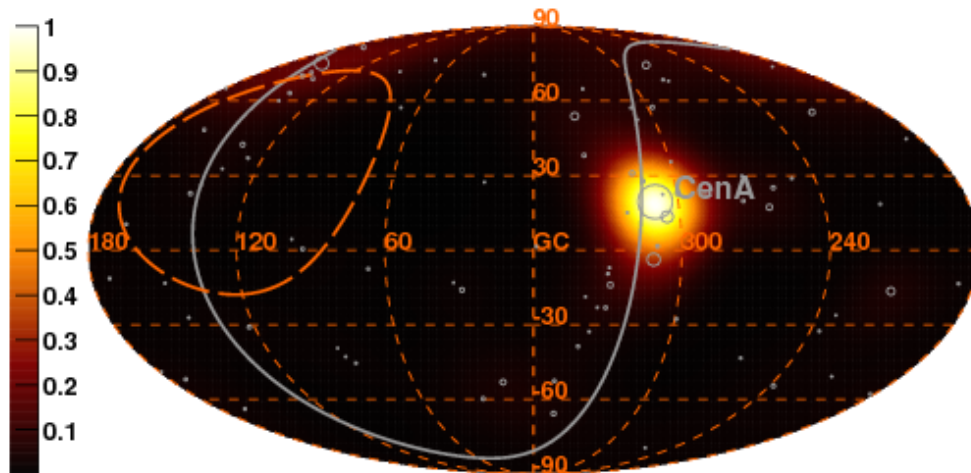
# Data-Model fit: angular smearing and anisotropic fraction



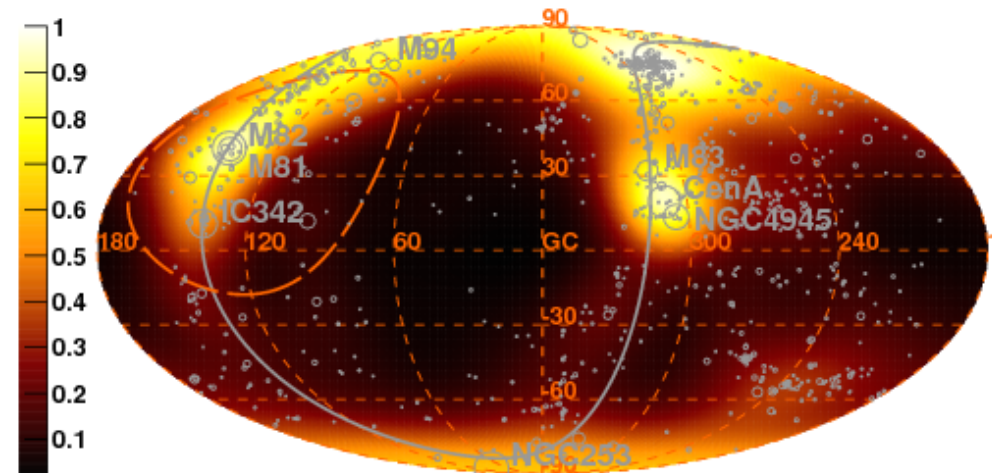


# Sky Model $(\text{flux}) \times (\text{attenuation model})_A \times (\text{angular smearing}), \text{ gal. coord.}$

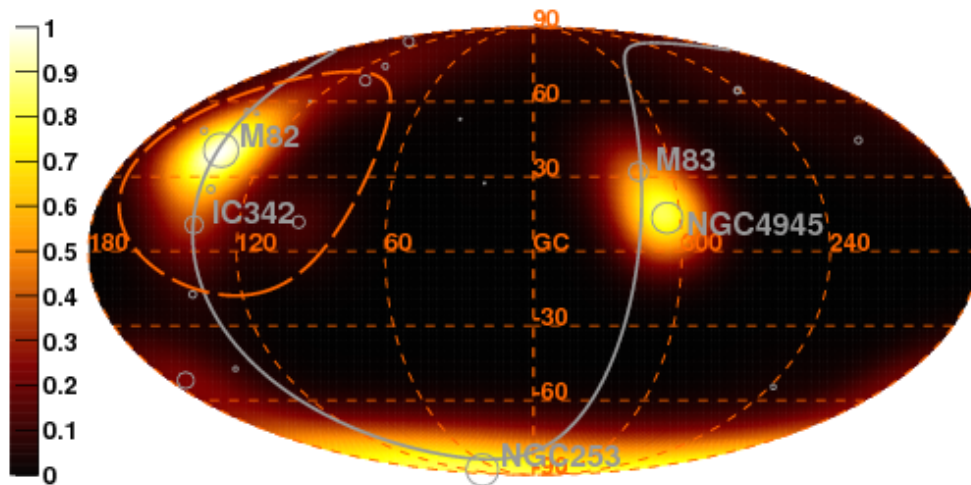
Model Flux Map - *Swift*-BAT -  $E > 39 \text{ EeV}$  - Sc. A



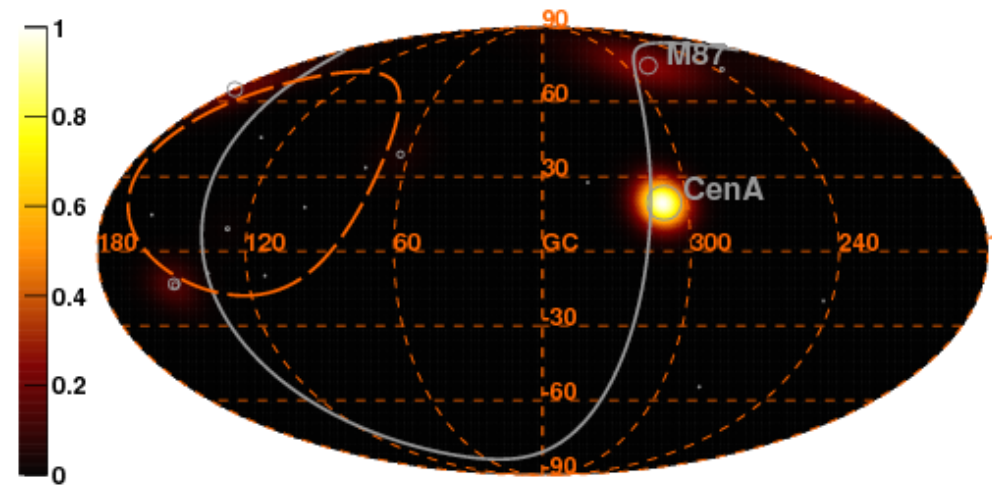
Model Flux Map - 2MRS  $> 1 \text{ Mpc}$  -  $E > 38 \text{ EeV}$  - Sc. A



Model Flux Map - Starburst galaxies -  $E > 39 \text{ EeV}$  - Sc. A



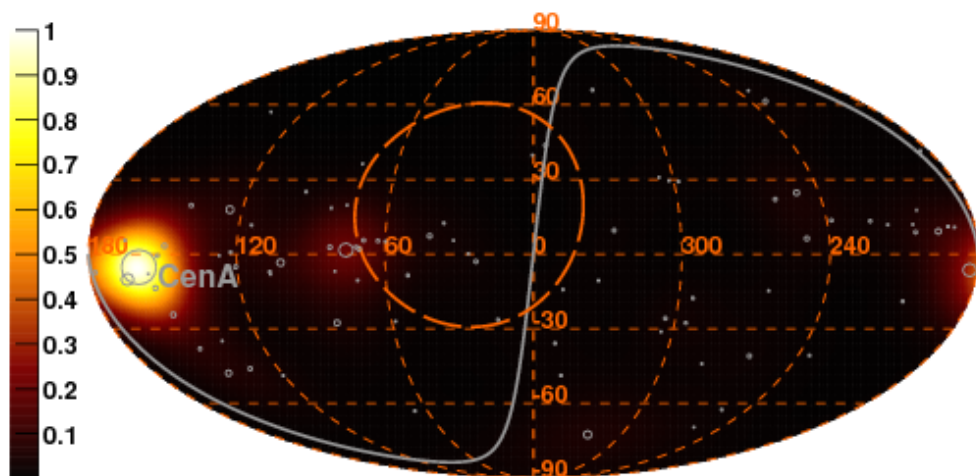
Model Flux Map - Active galactic nuclei -  $E > 60 \text{ EeV}$  - Sc. A



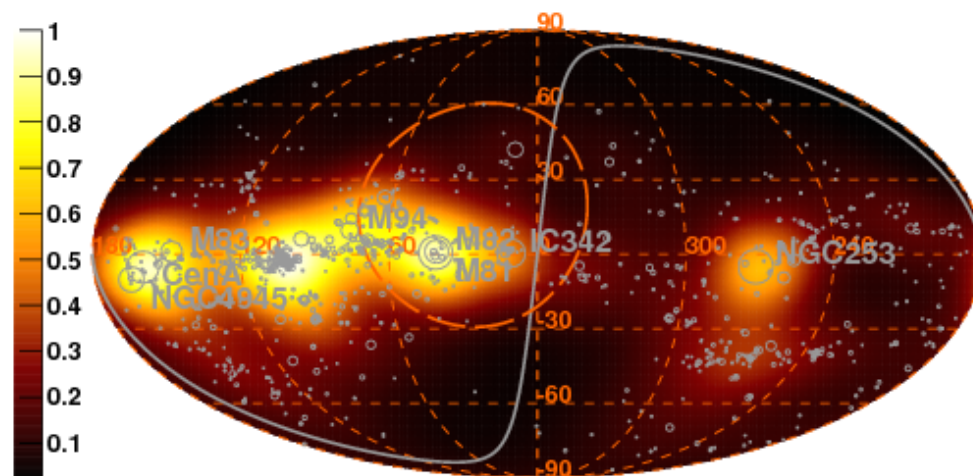
note region with zero exposure

# Sky Model $(\text{flux}) \times (\text{attenuation model})_A \times (\text{angular smearing}), \text{ super-gal. coord.}$

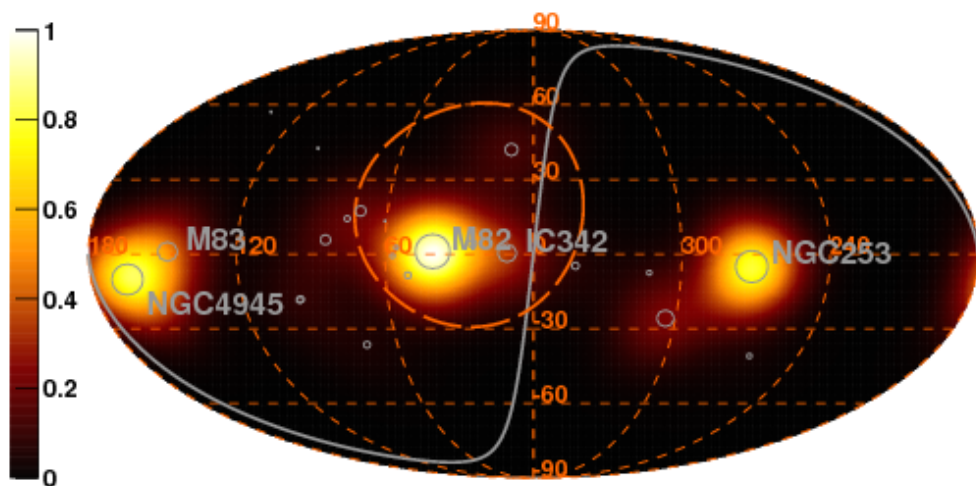
Model Flux Map - *Swift*-BAT -  $E > 39 \text{ EeV}$  - Sc. A



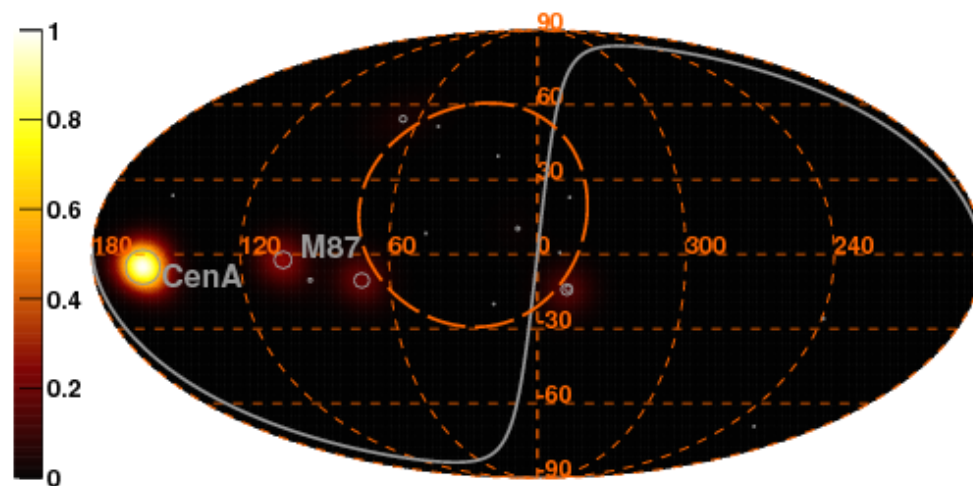
Model Flux Map - 2MRS  $> 1 \text{ Mpc}$  -  $E > 38 \text{ EeV}$  - Sc. A



Model Flux Map - Starburst galaxies -  $E > 39 \text{ EeV}$  - Sc. A



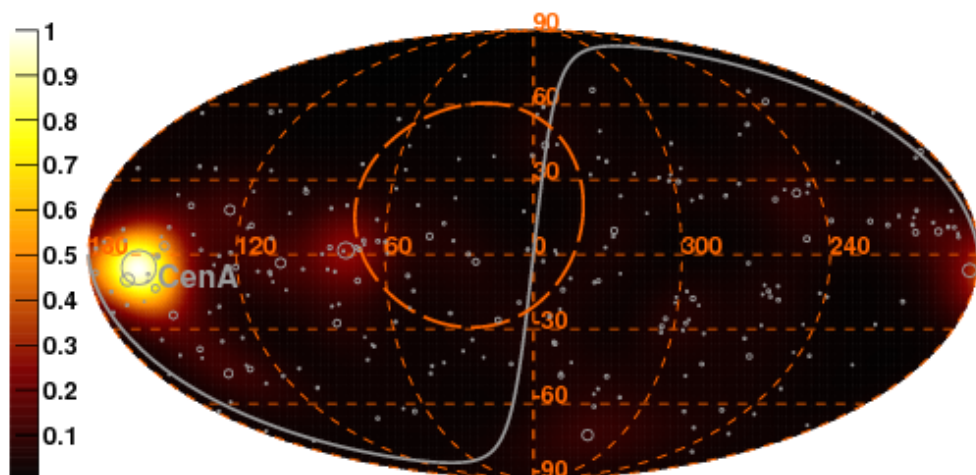
Model Flux Map - Active galactic nuclei -  $E > 60 \text{ EeV}$  - Sc. A



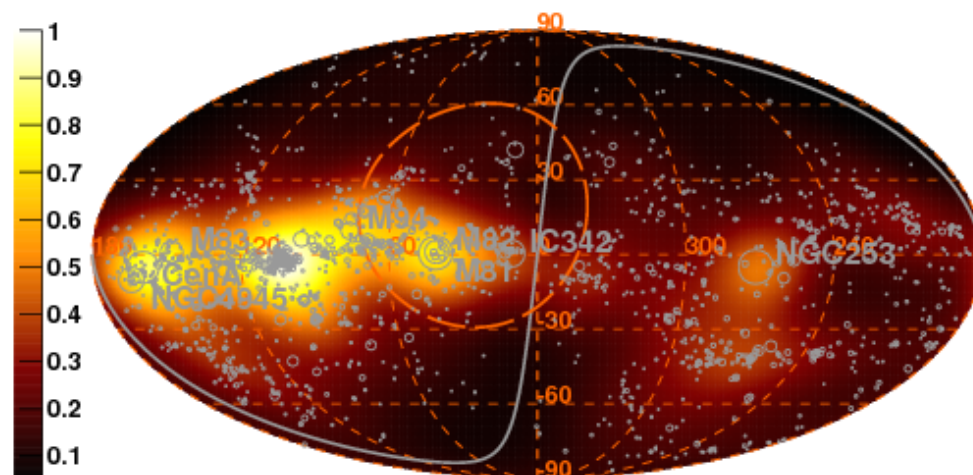
note region with zero exposure

# Sky Model $(\text{flux}) \times (\text{attenuation model})_B \times (\text{angular smearing}), \text{ super-gal. coord.}$

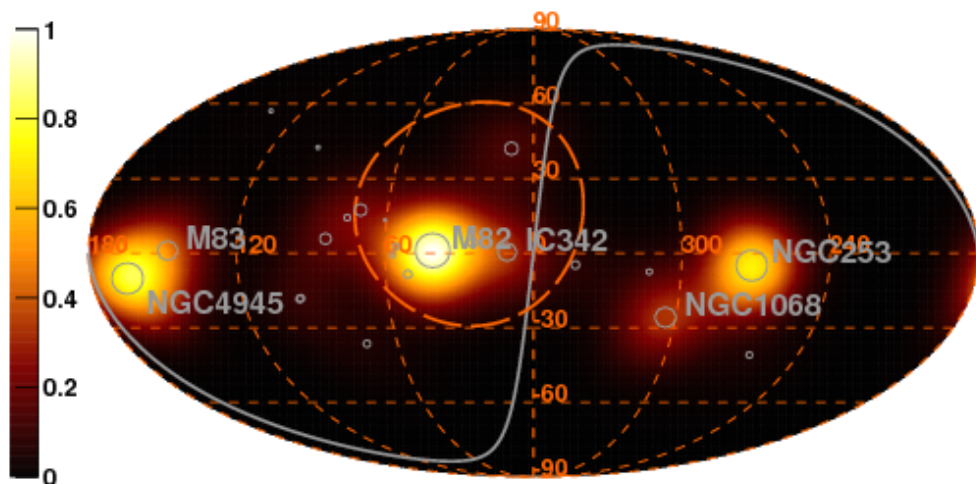
Model Flux Map - *Swift*-BAT -  $E > 39 \text{ EeV}$  - Sc. B



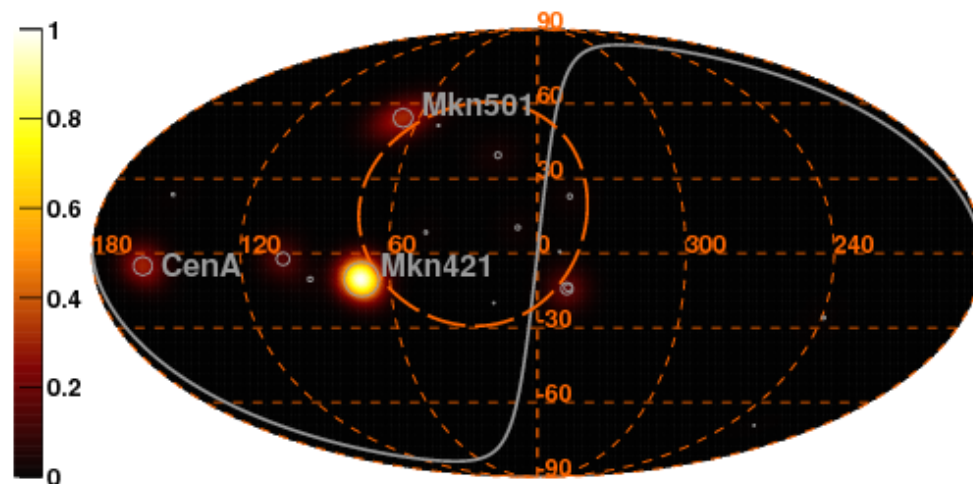
Model Flux Map - 2MRS  $> 1 \text{ Mpc}$  -  $E > 38 \text{ EeV}$  - Sc. B



Model Flux Map - Starburst galaxies -  $E > 39 \text{ EeV}$  - Sc. B

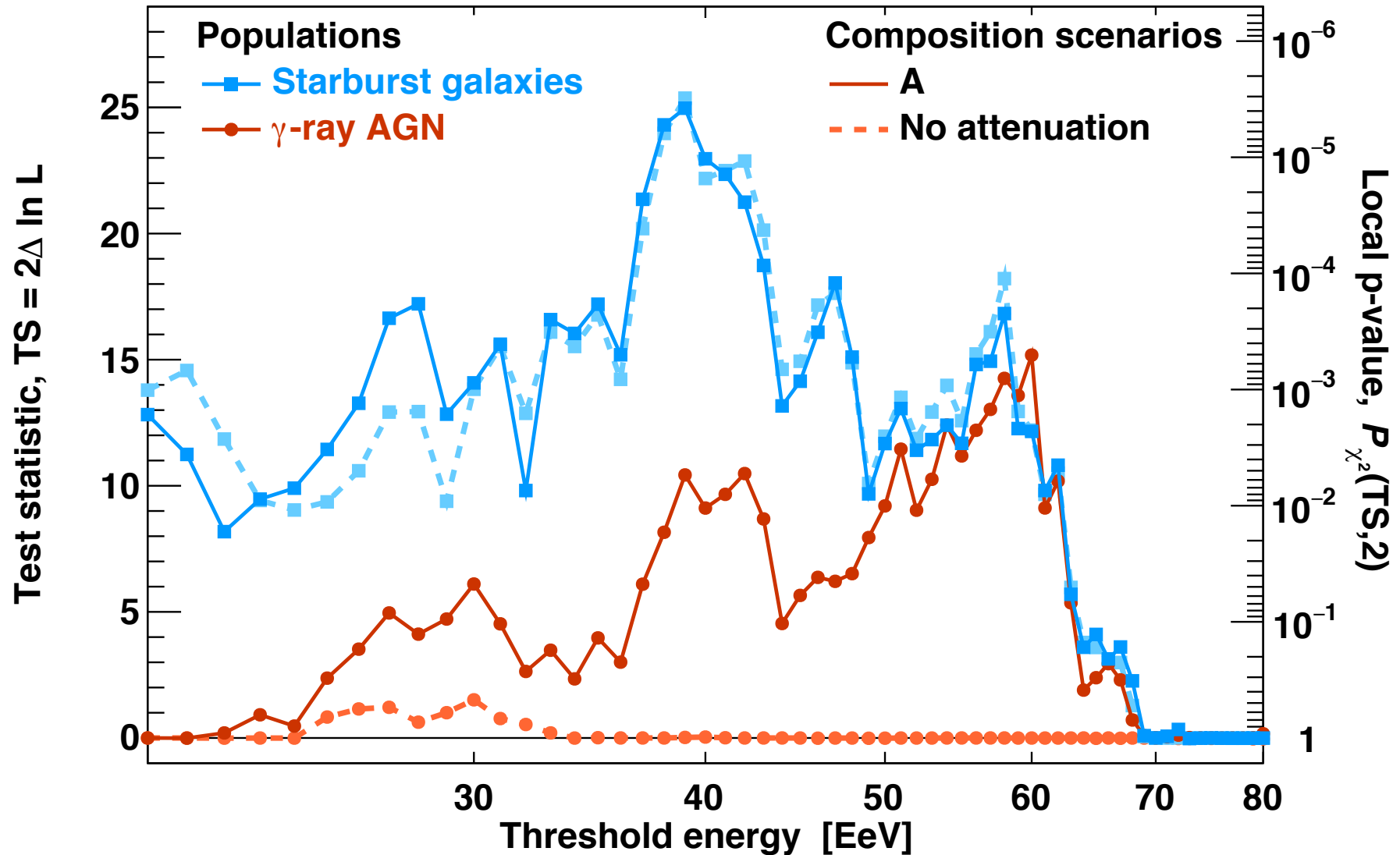


Model Flux Map - Active galactic nuclei -  $E > 60 \text{ EeV}$  - Sc. B



note region with zero exposure

# Test Statistic (TS) vs Energy



starburst model fits data better than isotropy, significance of  $4\sigma^*$ .

\*  $P_{\chi^2}(TS, 2)$  penalized for energy scan

# Detail of results of the sky models

A. Aab et al. [Auger Collab.] ApJ. Lett. **833** (2018) L29

Test hypothesis	Null hypothesis	Threshold energy <sup>a</sup>	TS	Local p-value $\mathcal{P}_{\chi^2}(\text{TS}, 2)$	Post-trial p-value	1-sided significance	AGN/other fraction	SBG fraction	Search radius
→ SBG + ISO	ISO	39 EeV	24.9	$3.8 \times 10^{-6}$	$3.6 \times 10^{-5}$	$4.0 \sigma$	N/A	9.7%	$12.9^\circ$
$\gamma$ AGN + SBG + ISO	$\gamma$ AGN + ISO	39 EeV	14.7	N/A	$1.3 \times 10^{-4}$	$3.7 \sigma$	0.7%	8.7%	$12.5^\circ$
→ $\gamma$ AGN + ISO	ISO	60 EeV	15.2	$5.1 \times 10^{-4}$	$3.1 \times 10^{-3}$	$2.7 \sigma$	6.7%	N/A	$6.9^\circ$
$\gamma$ AGN + SBG + ISO	SBG + ISO	60 EeV	3.0	N/A	0.08	$1.4 \sigma$	6.8%	0.0% <sup>b</sup>	$7.0^\circ$
<i>Swift</i> -BAT + ISO	ISO	39 EeV	18.2	$1.1 \times 10^{-4}$	$8.0 \times 10^{-4}$	$3.2 \sigma$	6.9%	N/A	$12.3^\circ$
<i>Swift</i> -BAT + SBG + ISO	<i>Swift</i> -BAT + ISO	39 EeV	7.8	N/A	$5.1 \times 10^{-3}$	$2.6 \sigma$	2.8%	7.1%	$12.6^\circ$
2MRS + ISO	ISO	38 EeV	15.1	$5.2 \times 10^{-4}$	$3.3 \times 10^{-3}$	$2.7 \sigma$	15.8%	N/A	$13.2^\circ$
2MRS + SBG + ISO	2MRS + ISO	39 EeV	10.4	N/A	$1.3 \times 10^{-3}$	$3.0 \sigma$	1.1%	8.9%	$12.6^\circ$

<sup>a</sup> For composite model studies, no scan over the threshold energy is performed.

<sup>b</sup> Maximum TS reached at the boundary of the parameter space.

ISO: isotropic model.

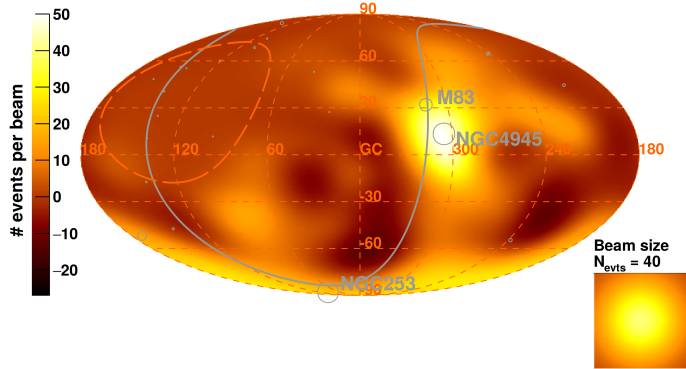
starburst model fits data better than isotropy, significance of  $4 \sigma^*$ .

\*  $\mathcal{P}_{\chi^2}(\text{TS}, 2)$  penalized for energy scan

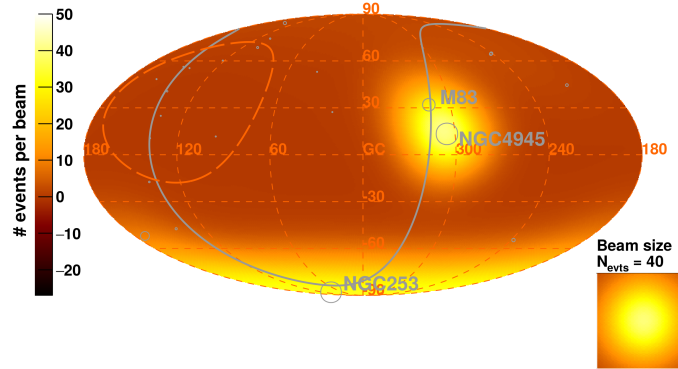
# Data vs Model for SBG and $\gamma$ AGN (galactic coords)

## top: starburst galaxies

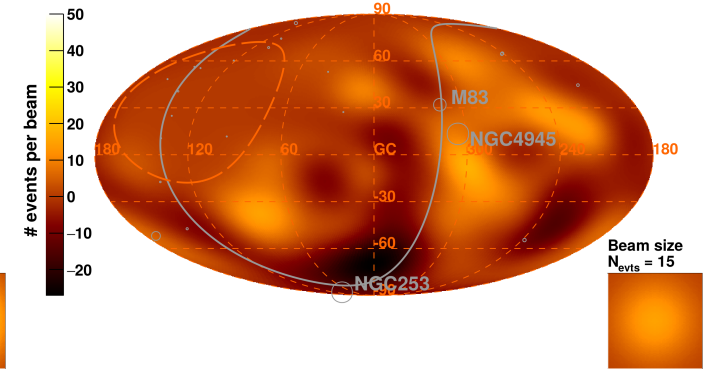
Observed Excess Map -  $E > 39$  EeV



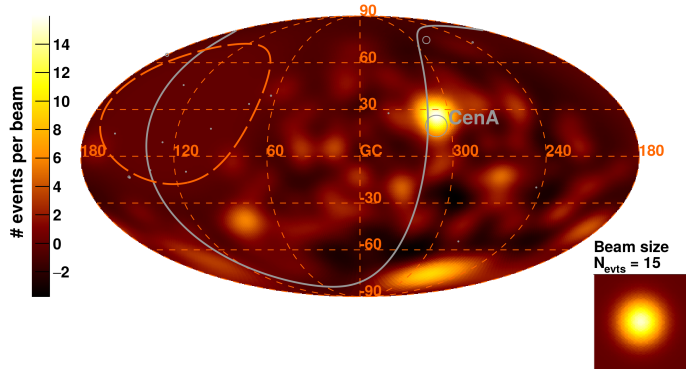
Model Excess Map - Starburst galaxies -  $E > 39$  EeV



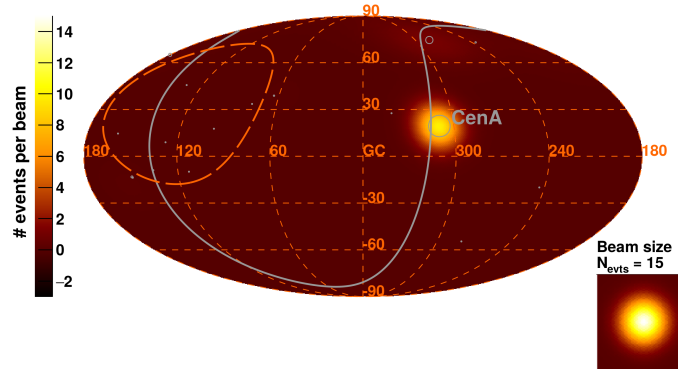
Residual Excess Map - Starburst galaxies -  $E > 39$  EeV



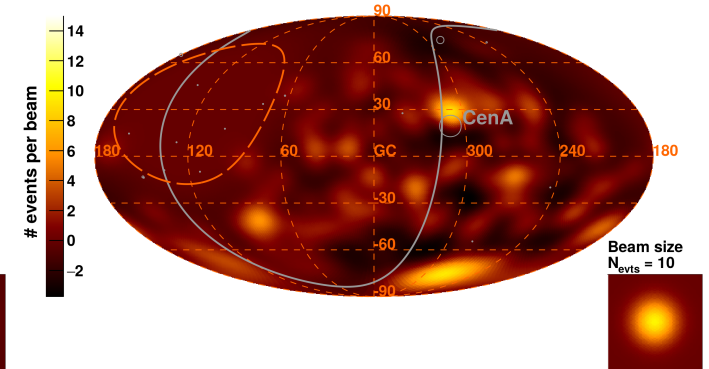
Observed Excess Map -  $E > 60$  EeV



Model Excess Map - Active galactic nuclei -  $E > 60$  EeV



Residual Excess Map - Active galactic nuclei -  $E > 60$  EeV

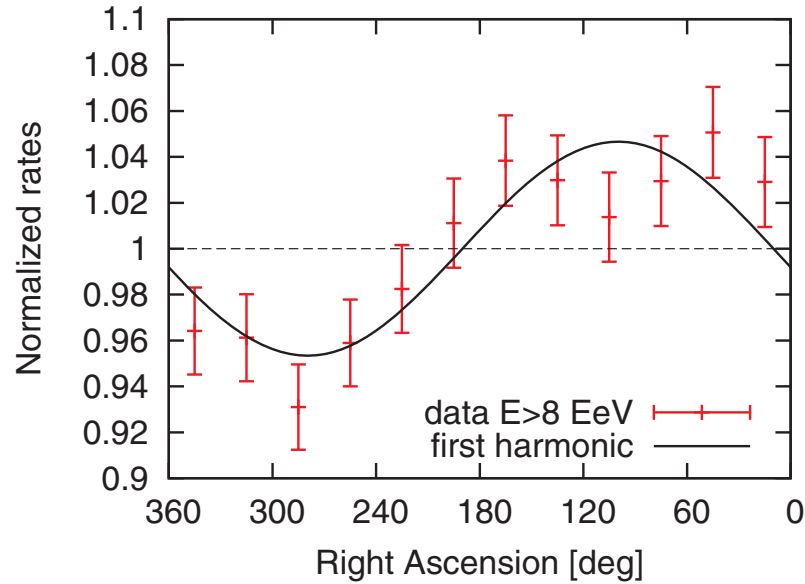


## bottom: $\gamma$ AGN

All are “excess” maps: best-fit isotropic component is subtracted.

# Observation of Dipolar Anisotropy above 8 EeV

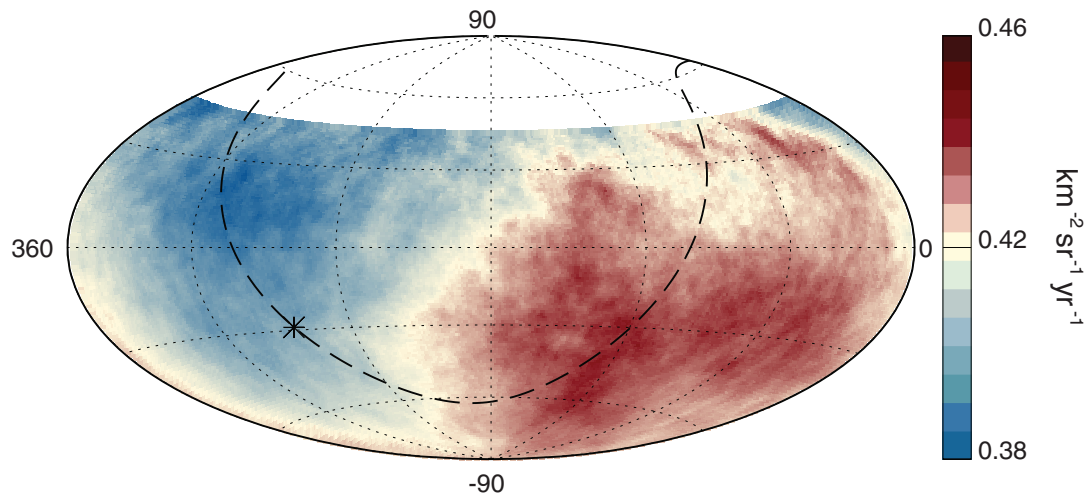
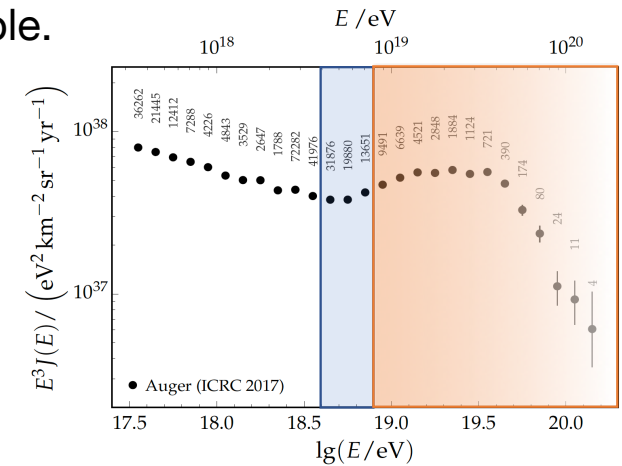
A. Aab et al. [Auger Collab.] Science **357** (2017) 1266



## Harmonic Analysis in right ascension (RA)

$E$ [EeV]	events	amplitude $r$	phase [deg.]	$P(\geq r)$
4-8	81701	$0.005^{+0.006}_{-0.002}$	$80 \pm 60$	0.60
> 8	32187	$0.047^{+0.008}_{-0.007}$	$100 \pm 10$	$2.6 \times 10^{-8}$

Significant modulation  $5.2\sigma$   
very close to a pure dipole.



## 3D dipole above 8 EeV

$(\alpha, \delta) = (100^\circ, -24^\circ)$ , amplitude  $6.5^{+1.3}_{-0.9} \%$

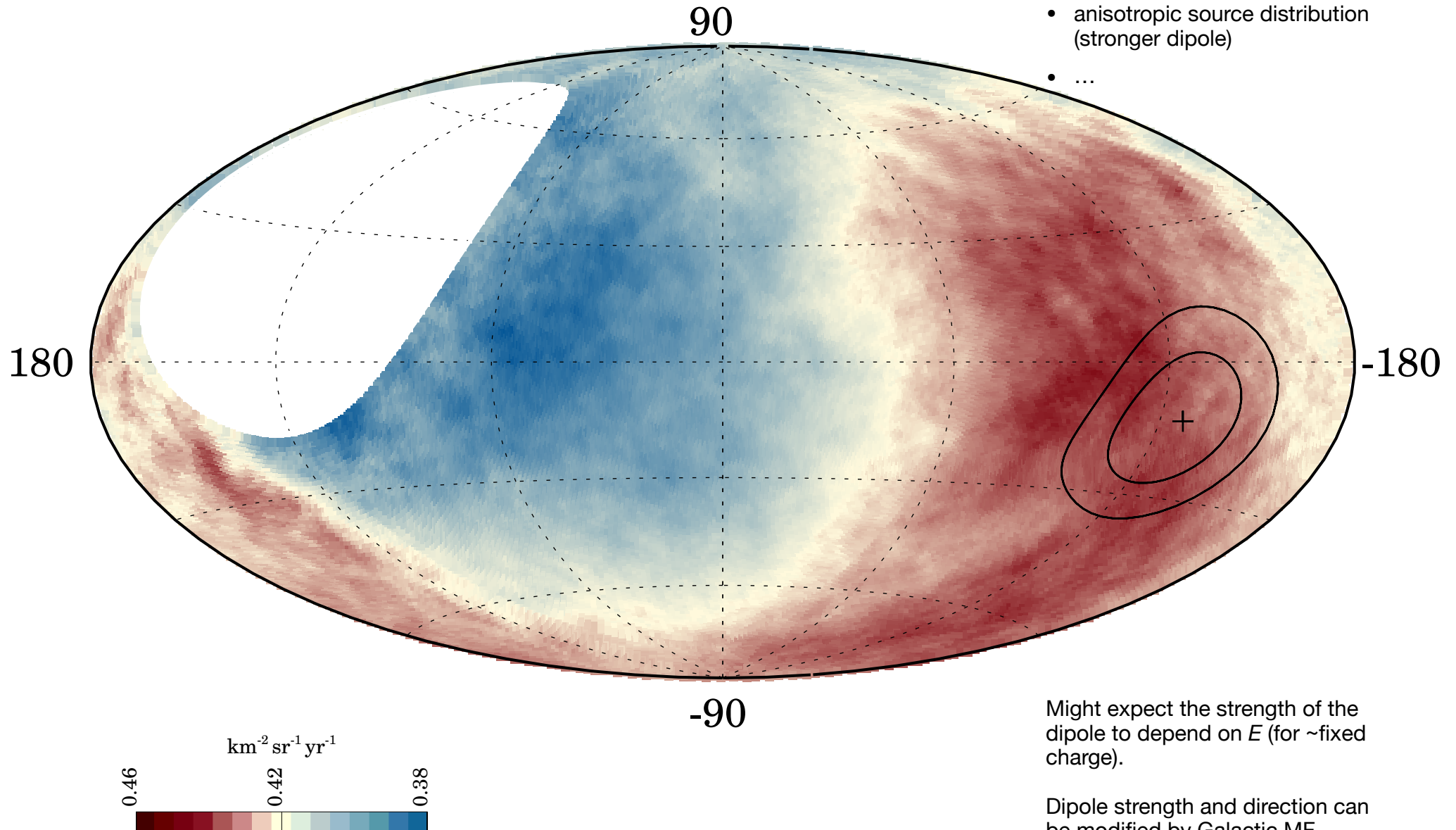


# Dipole in galactic coordinates

Strong evidence for extragalactic origin at these energies  
- dipole direction 125 degrees from GC.

Dipole could be the result of

- single source + diffusion
- isotropic source distribution (some sources always closer)
- anisotropic source distribution (stronger dipole)
- ...



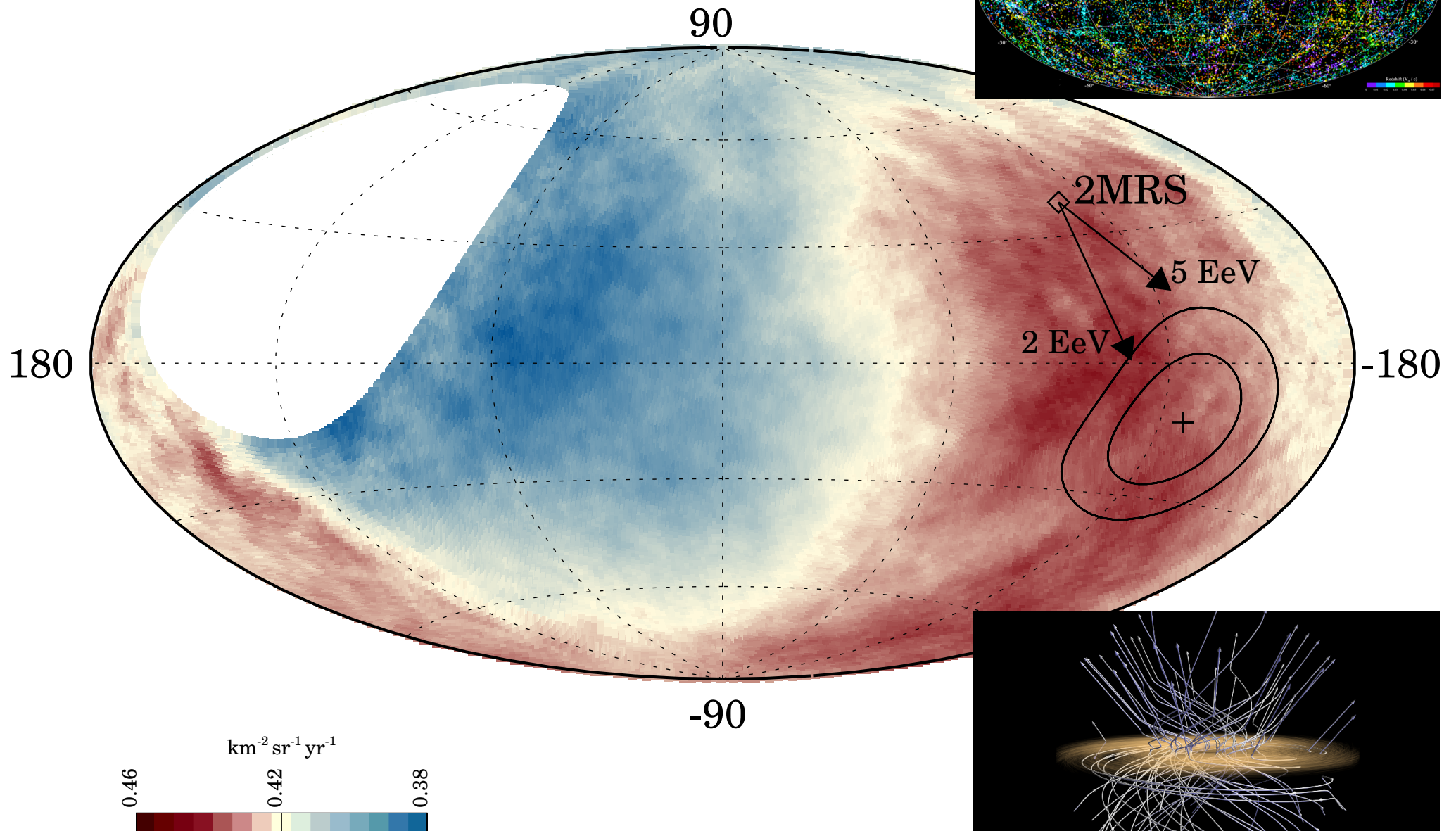
Might expect the strength of the dipole to depend on  $E$  (for  $\sim$ fixed charge).

Dipole strength and direction can be modified by Galactic MF.



# Dipole in galactic coordinates

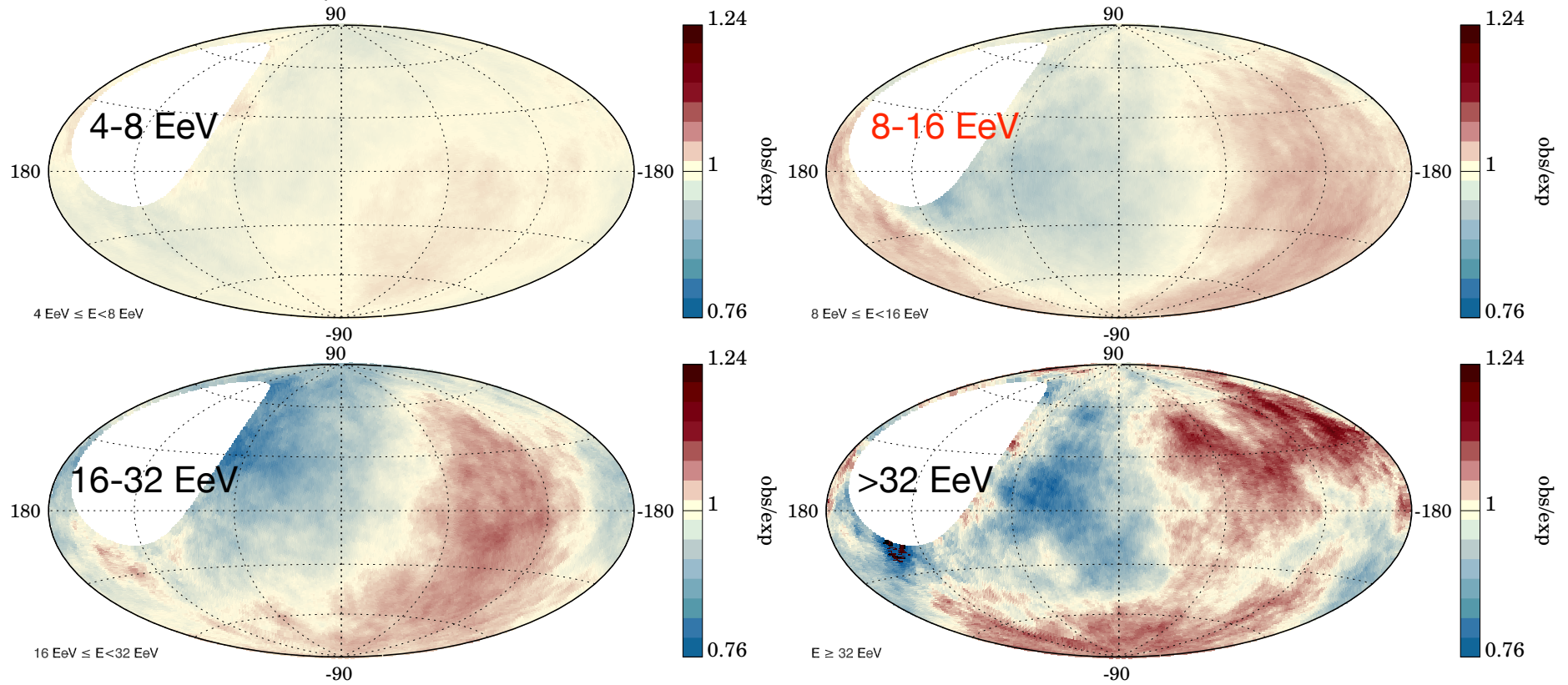
Strong evidence for extragalactic origin at these energies  
- dipole direction 125 degrees from GC.



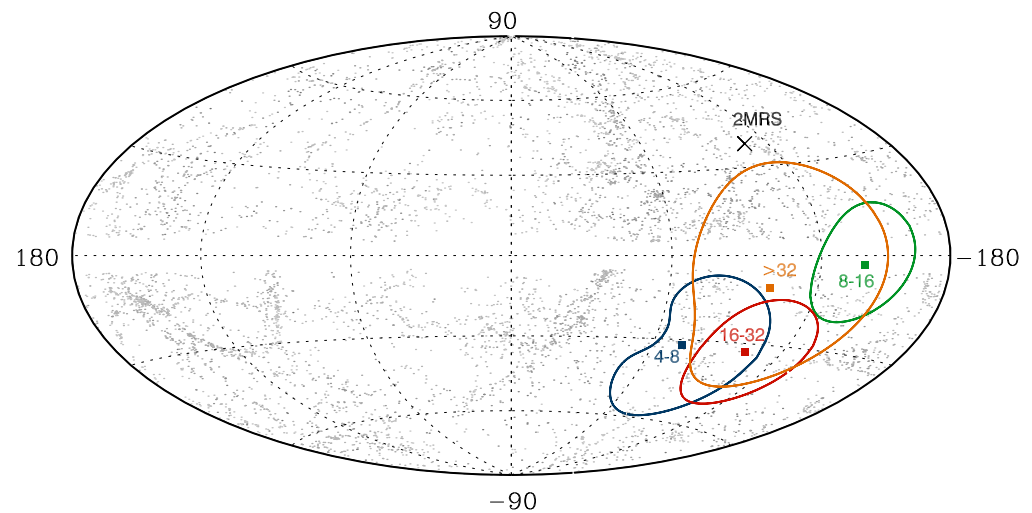
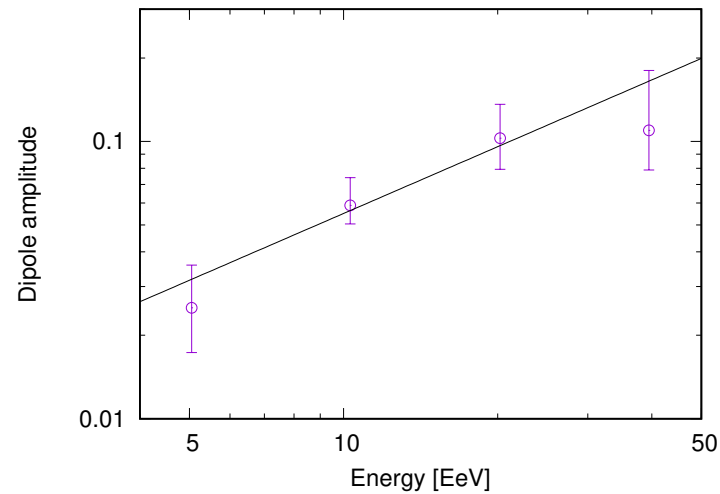
See other studies, e.g. Globus & Piran Ap.J. (2017)  
- Noemie's talk this afternoon!

# Dipole - some energy dependence?

same fractional excess scale on each plot



(only 8-16 EeV bin has a statistically significant result)

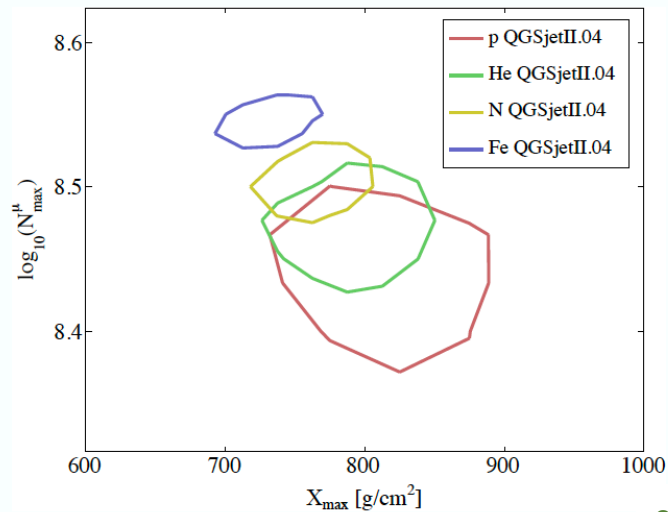


# Upgrade to the Auger Observatory - AugerPrime

- mass composition information for every event

To increase exposure with composition sensitive data Surface array needed!

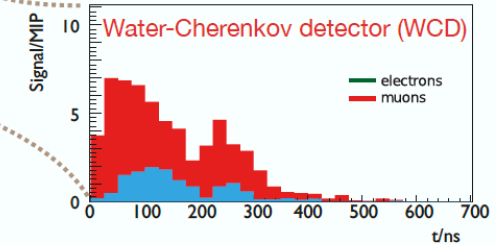
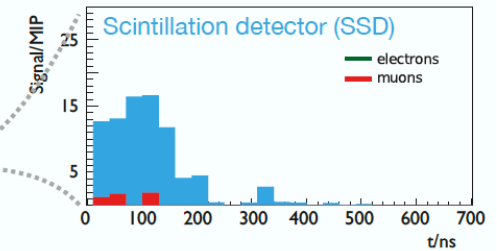
Duty cycle: 100% (SD) vs 15% (FD)



(AugerPrime design report 1604.03637)



complementarity of light responses used to discriminate e.m. and muonic components



$$S_{\mu, \text{WCD}} = a S_{\text{WCD}} + b S_{\text{SSD}}$$

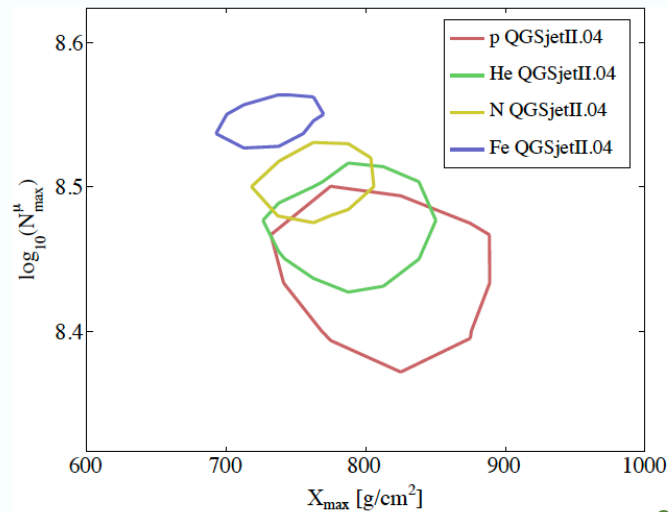
$$S_{\text{em}, \text{WCD}} = c S_{\text{WCD}} + d S_{\text{SSD}}$$

# Upgrade to the Auger Observatory - AugerPrime

- mass composition information for every event

To increase exposure with composition sensitive data Surface array needed!

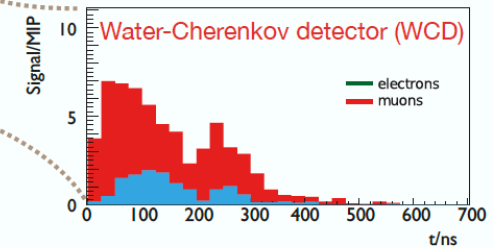
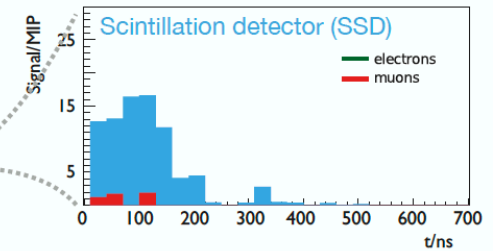
Duty cycle: 100% (SD) vs 15% (FD)



(AugerPrime design report 1604.03637)



complementarity of light responses used to discriminate e.m. and muonic components



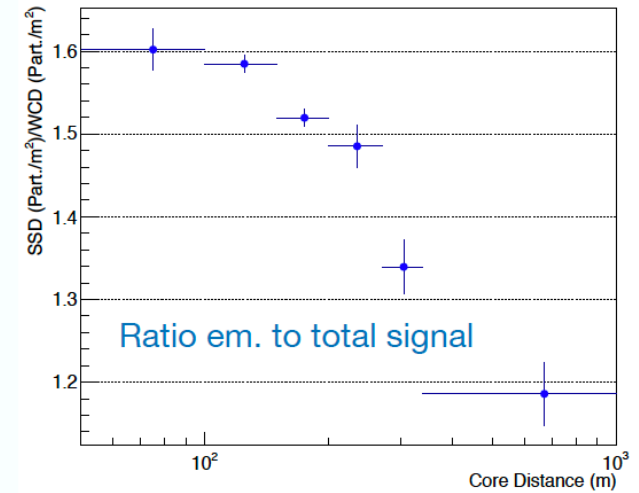
## Moreover

- Upgraded and faster electronics
- Extension of the dynamic range
- Cross check with underground buried AMIGA detectors
- Extension of the FD duty cycle

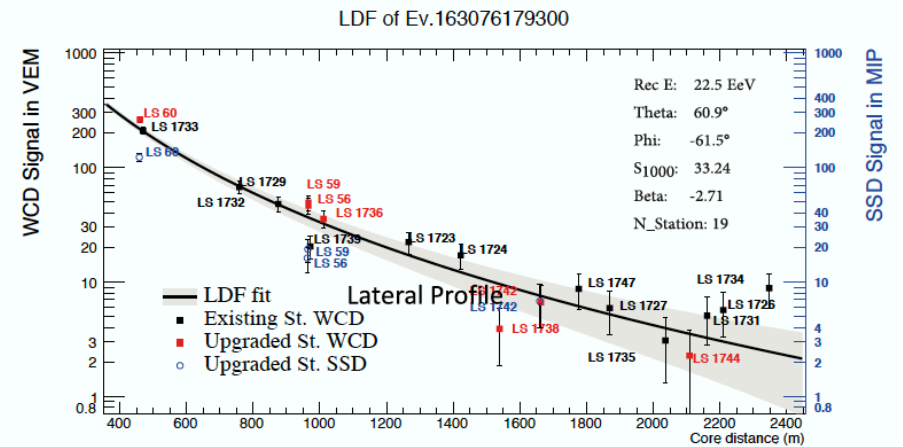
# Upgrade to the Auger Observatory - AugerPrime

## Status and plans for AugerPrime

- Composition measurement at  $10^{20}$  eV
- Composition selected anisotropy studies
- Particle physics with air showers



2016: engineering array; 12 stations  
 2018-19: deployment  
 2019-25: data taking (40,000 km<sup>2</sup> sr yr)



# Summary

- Spectrum and composition
  - highest exposure measurement of **spectrum** , strong flux suppression
  - **Composition** with FD and SD
    - light composition at ankle
    - mixed composition at UHE
    - hints of galactic Fe at lowest energies?
  - compatible with rigidity-dependent cut-off at sources
- Anisotropy
  - observation of **dipole anisotropy**  $E > 8$  EeV
  - **indication** of **medium-scale anisotropy**,  $E > 39$  EeV
- Other results (no time)
  - UHE Neutrino and gamma-ray limits constraining proton-dominated sources
  - Hadronic interactions (normal UHE cross-sections, muon deficits in models)
- **AugerPrime Upgrade**

